# Web-based supporting materials for "Dynamic predictions of kidney graft survival in the presence of longitudinal outliers" by

Özgür Asar[1*], Marie-Cécile Fournier[2] and Etienne Dantan[2]

[1]Department of Biostatistics and Medical Informatics, Acıbadem Mehmet Ali Aydınlar University, İstanbul, Turkey.

[2]INSERM UMR 1246 - SPHERE, Nantes University, Tours University, Nantes, France.

* ozgur.asar@acibadem.edu.tr | ozgurasarstat@gmail.com

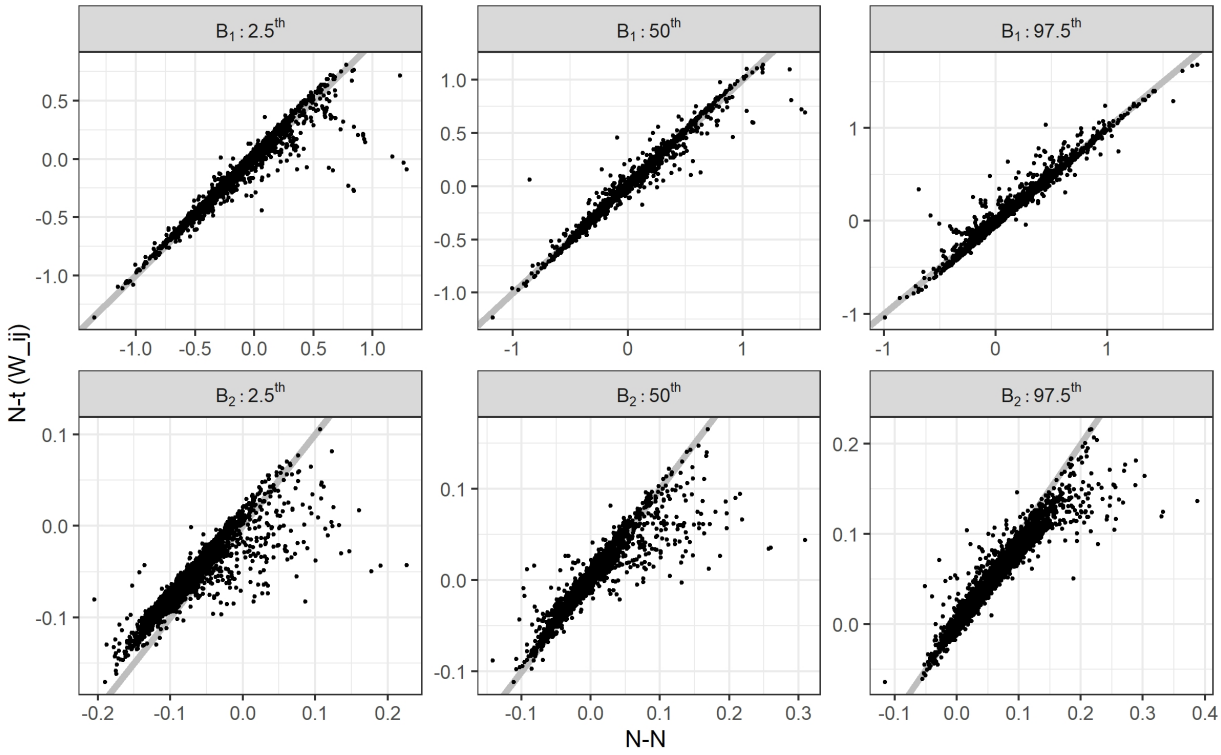


Figure 1: Scatter-plots of posterior quantiles (2.5th: left panel, 50th: mid, 97.5th: right) for $B_{1i}$ (upper panel) and $B_{2i}$ (lower panel) based on the learning data-set. x-axis is the $N-N$ model, y-axis the $N-t$ ($W_{ij}$). Gray lines are $x=y$ lines.

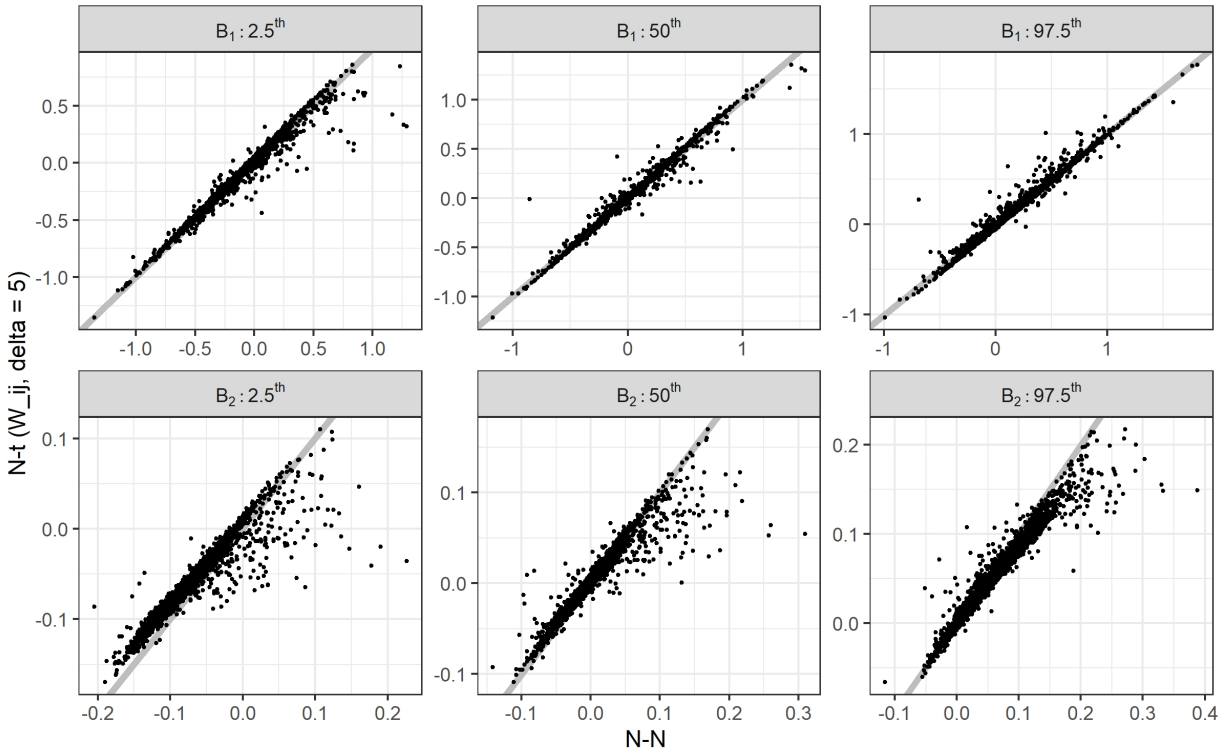


Figure 2: Scatter-plots of posterior quantiles (2.5th: left panel, 50th: mid, 97.5th: right) for $B_{1i}$ (upper panel) and $B_{2i}$ (lower panel) based on the learning data-set. x-axis is the $N-N$ model, y-axis the $N-t$ ($W_{ij}, \delta = 5$). Gray lines are $x = y$ lines.

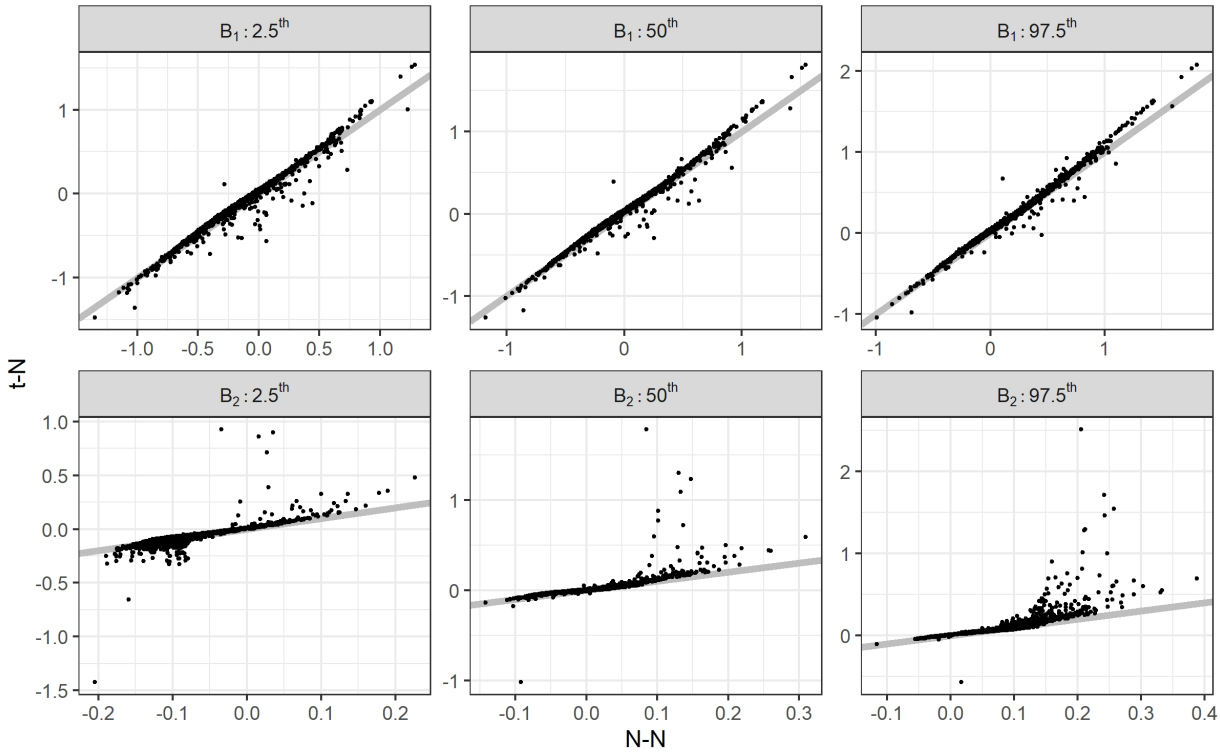


Figure 3: Scatter-plots of posterior quantiles (2.5th: left panel, 50th: mid, 97.5th: right) for $B_{1i}$ (upper panel) and $B_{2i}$ (lower panel) based on the learning data-set. x-axis is the $N - N$ model, y-axis the $t - N$. Gray lines are $x = y$ lines.

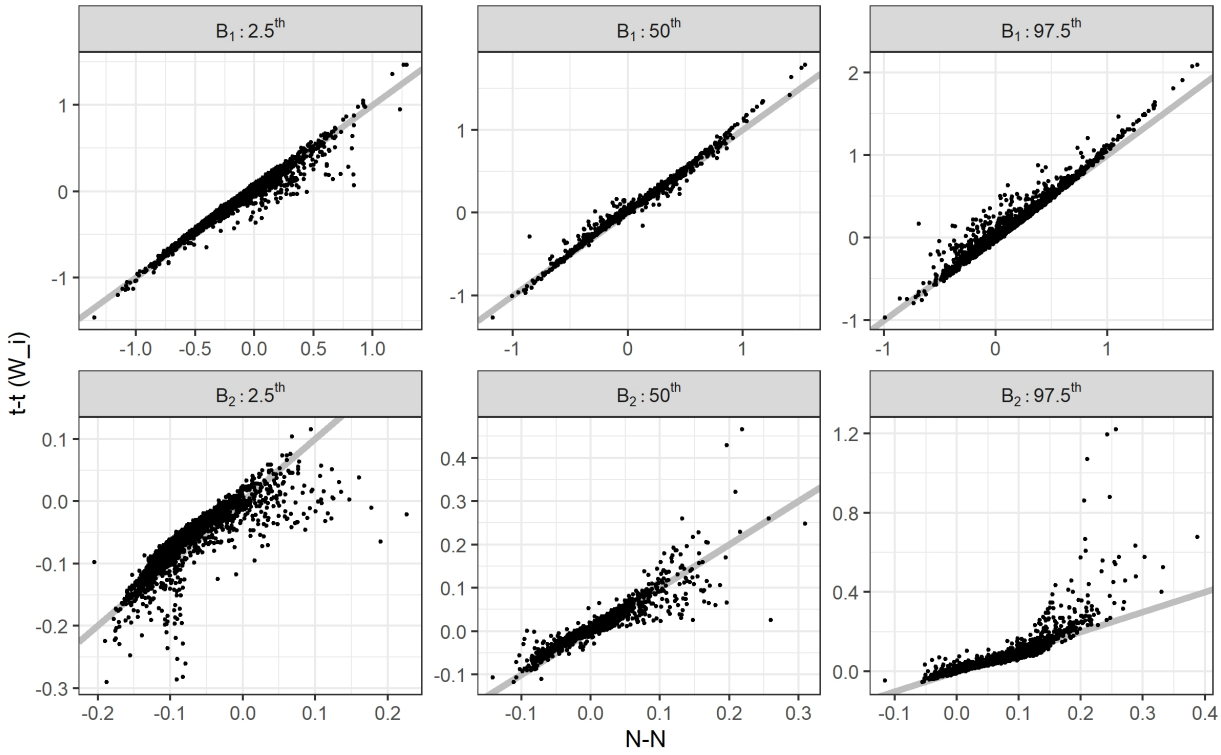


Figure 4: Scatter-plots of posterior quantiles (2.5th: left panel, 50th: mid, 97.5th: right) for $B_{1i}$ (upper panel) and $B_{2i}$ (lower panel) based on the learning data-set. x-axis is the $N - N$ model, y-axis the $t - t$ ($W_i$). Gray lines are $x = y$ lines.

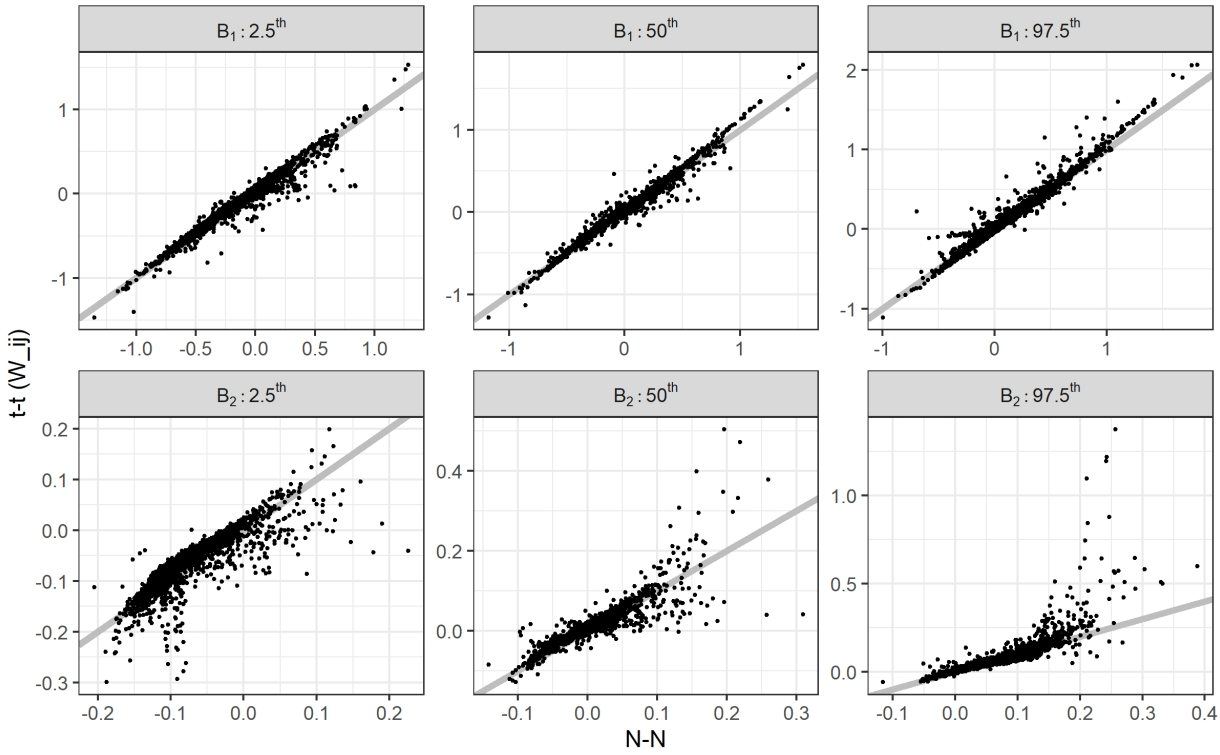


Figure 5: Scatter-plots of posterior quantiles (2.5th: left panel, 50th: mid, 97.5th: right) for $B_{1i}$ (upper panel) and $B_{2i}$ (lower panel) based on the learning data-set. x-axis is the $N - N$ model, y-axis the $t - t$ ($W_{ij}$). Gray lines are $x = y$ lines.

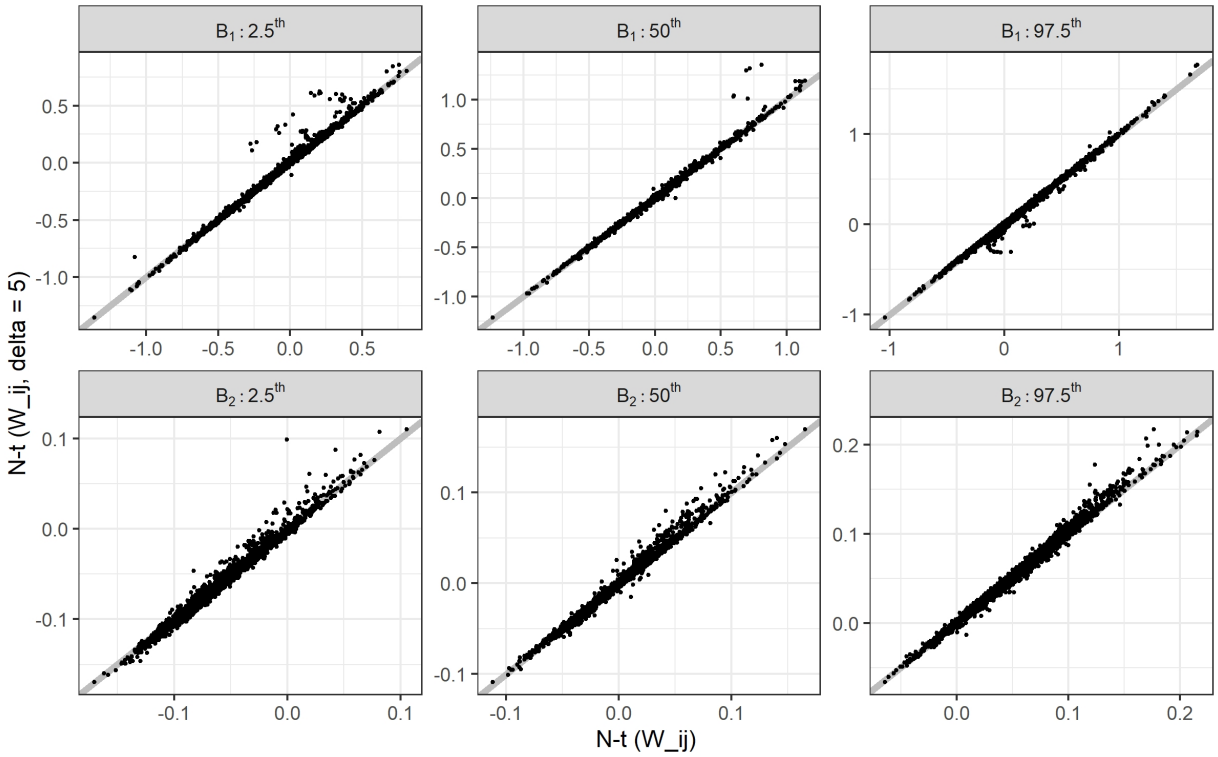


Figure 6: Scatter-plots of posterior quantiles (2.5th: left panel, 50th: mid, 97.5th: right) for $B_{1i}$ (upper panel) and $B_{2i}$ (lower panel) based on the learning data-set. x-axis is the $N-t$ $(W_{ij})$ model, y-axis the $N-t$ $(W_{ij}, \delta = 5)$. Gray lines are $x = y$ lines.

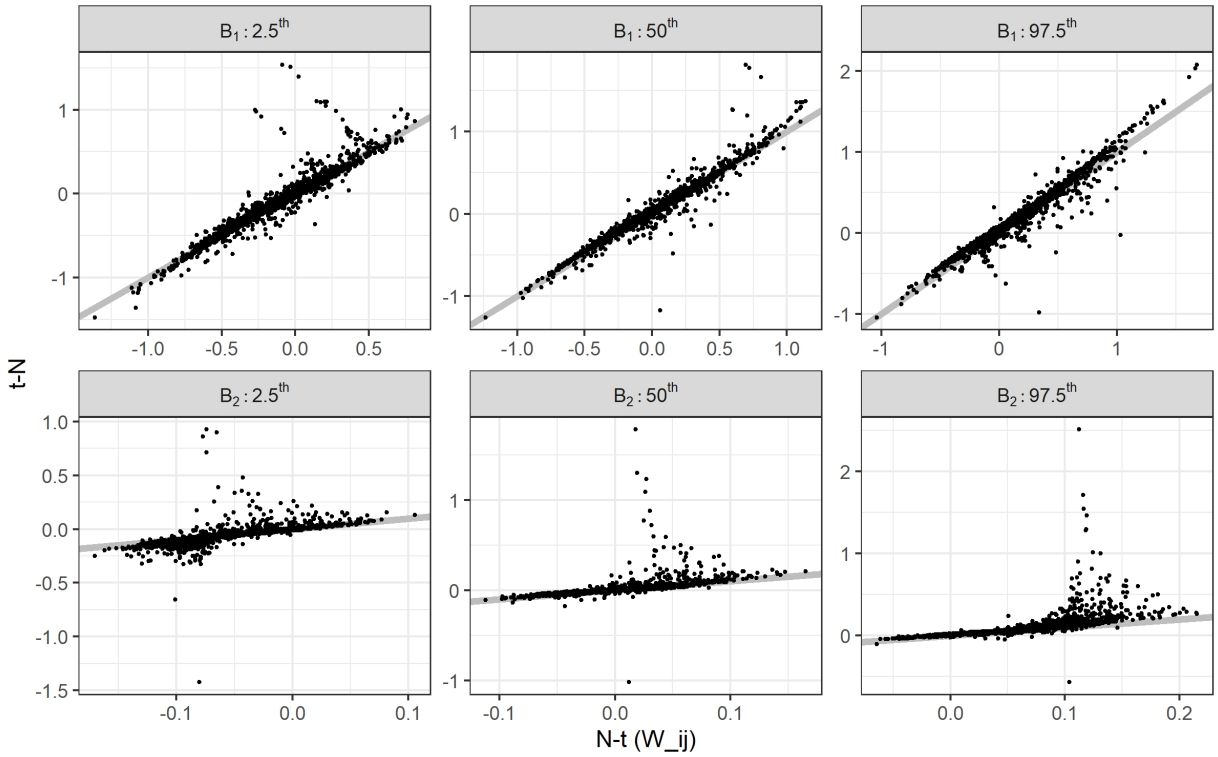


Figure 7: Scatter-plots of posterior quantiles (2.5th: left panel, 50th: mid, 97.5th: right) for $B_{1i}$ (upper panel) and $B_{2i}$ (lower panel) based on the learning data-set. x-axis is the $N-t$ ($W_{ij}$) model, y-axis the $t-N$. Gray lines are $x=y$ lines.

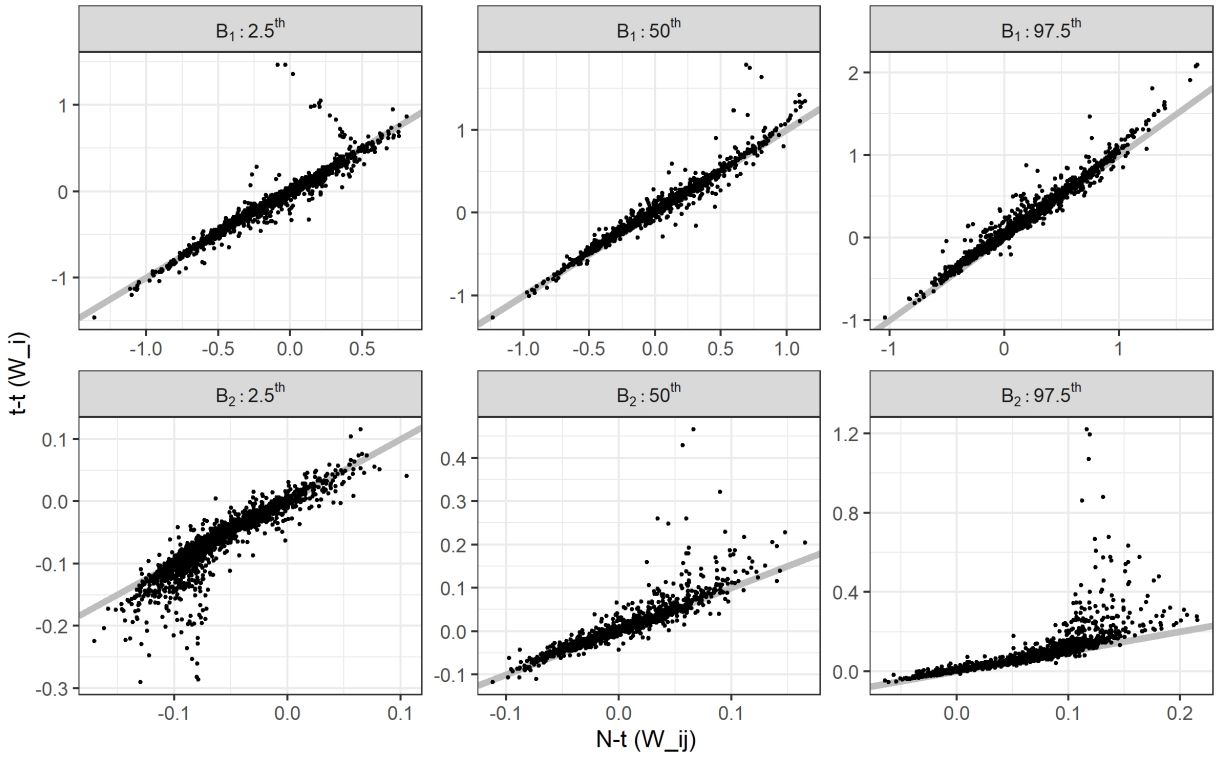


Figure 8: Scatter-plots of posterior quantiles (2.5th: left panel, 50th: mid, 97.5th: right) for $B_{1i}$ (upper panel) and $B_{2i}$ (lower panel) based on the learning data-set. x-axis is the $N-t$ ($W_{ij}$) model, y-axis the $t-t$ ($W_i$). Gray lines are $x=y$ lines.

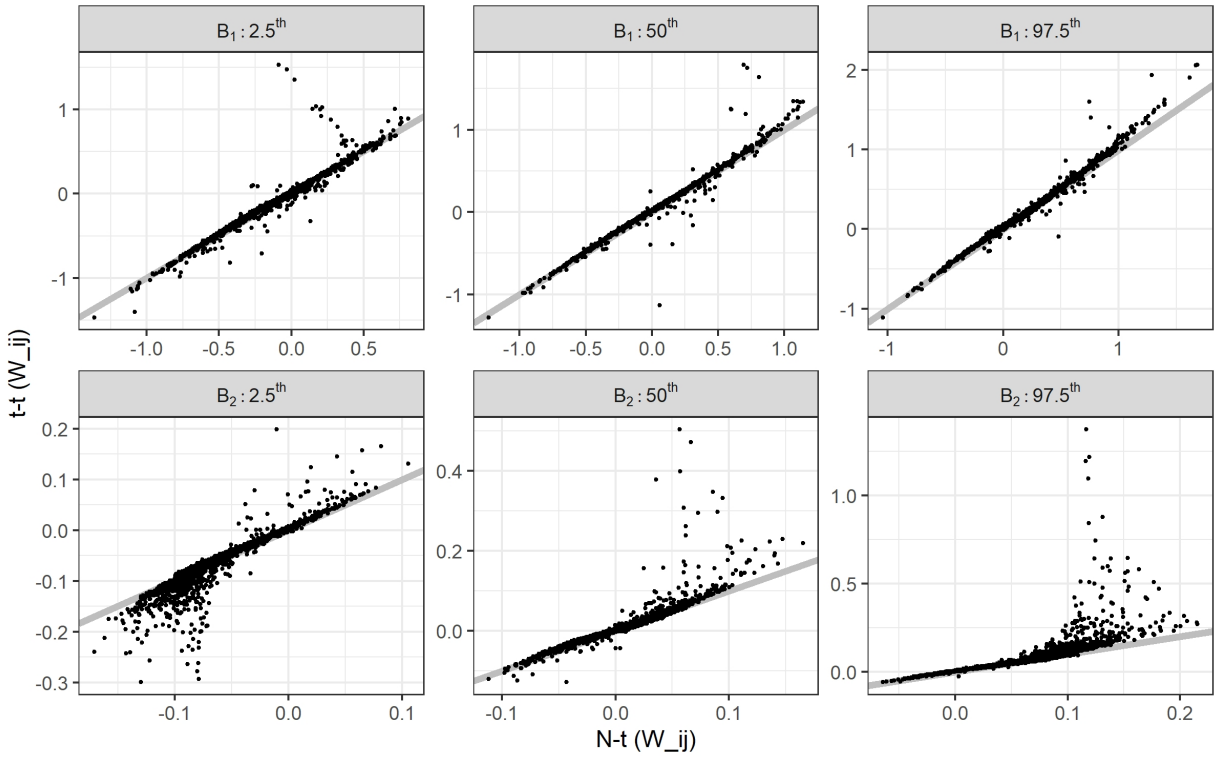


Figure 9: Scatter-plots of posterior quantiles (2.5th: left panel, 50th: mid, 97.5th: right) for $B_{1i}$ (upper panel) and $B_{2i}$ (lower panel) based on the learning data-set. x-axis is the $N-t$ $(W_{ij})$ model, y-axis the $t-t$ $(W_{ij})$. Gray lines are $x=y$ lines.

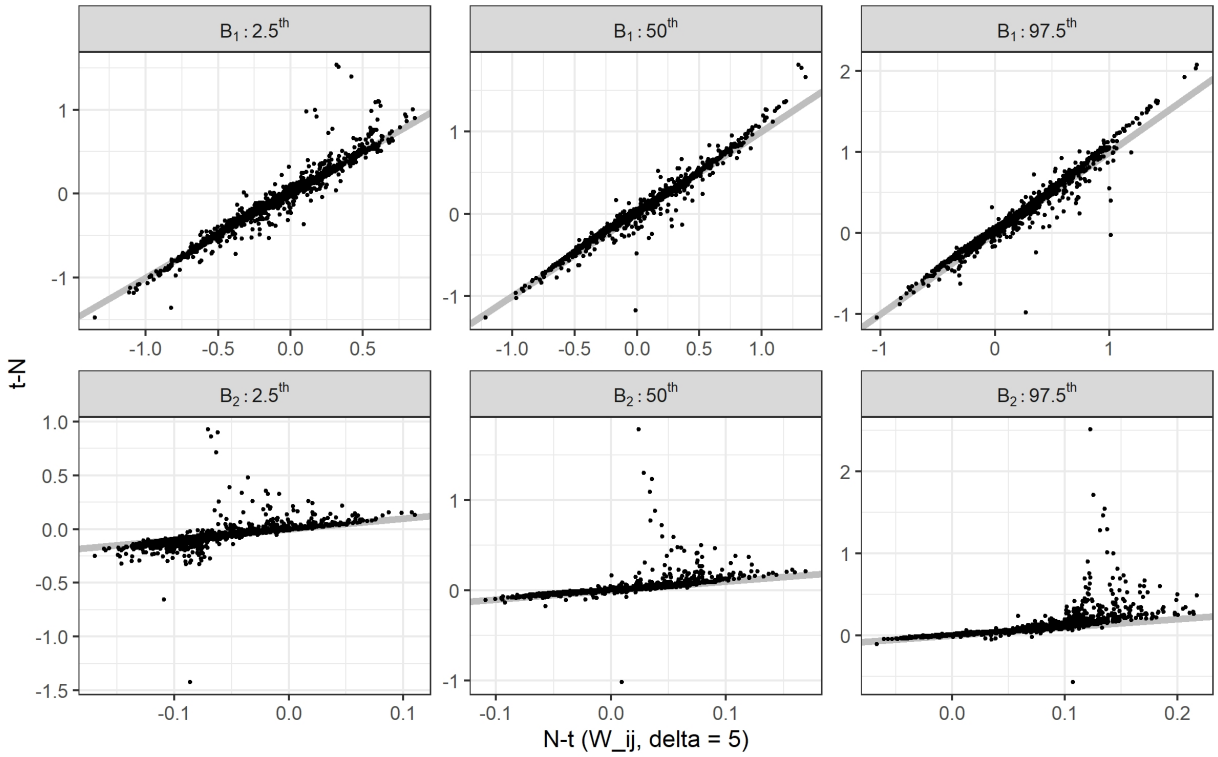


Figure 10: Scatter-plots of posterior quantiles (2.5th: left panel, 50th: mid, 97.5th: right) for $B_{1i}$ (upper panel) and $B_{2i}$ (lower panel) based on the learning data-set. x-axis is the $N-t$ $(W_{ij}, \delta = 5)$ model, y-axis the $t-N$. Gray lines are $x = y$ lines.

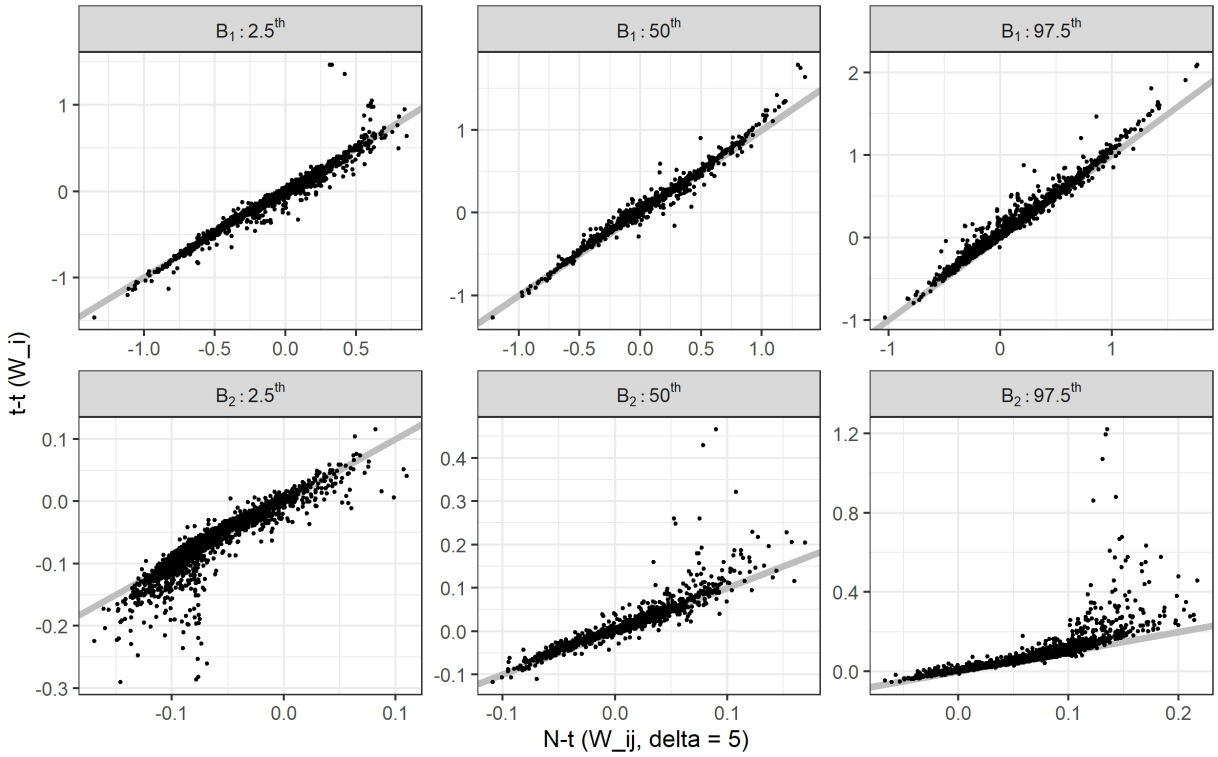


Figure 11: Scatter-plots of posterior quantiles (2.5th: left panel, 50th: mid, 97.5th: right) for $B_{1i}$ (upper panel) and $B_{2i}$ (lower panel) based on the learning data-set. x-axis is the $N-t$ $(W_{ij}, \delta = 5)$ model, y-axis the $t-t$ $(W_i)$. Gray lines are $x = y$ lines.

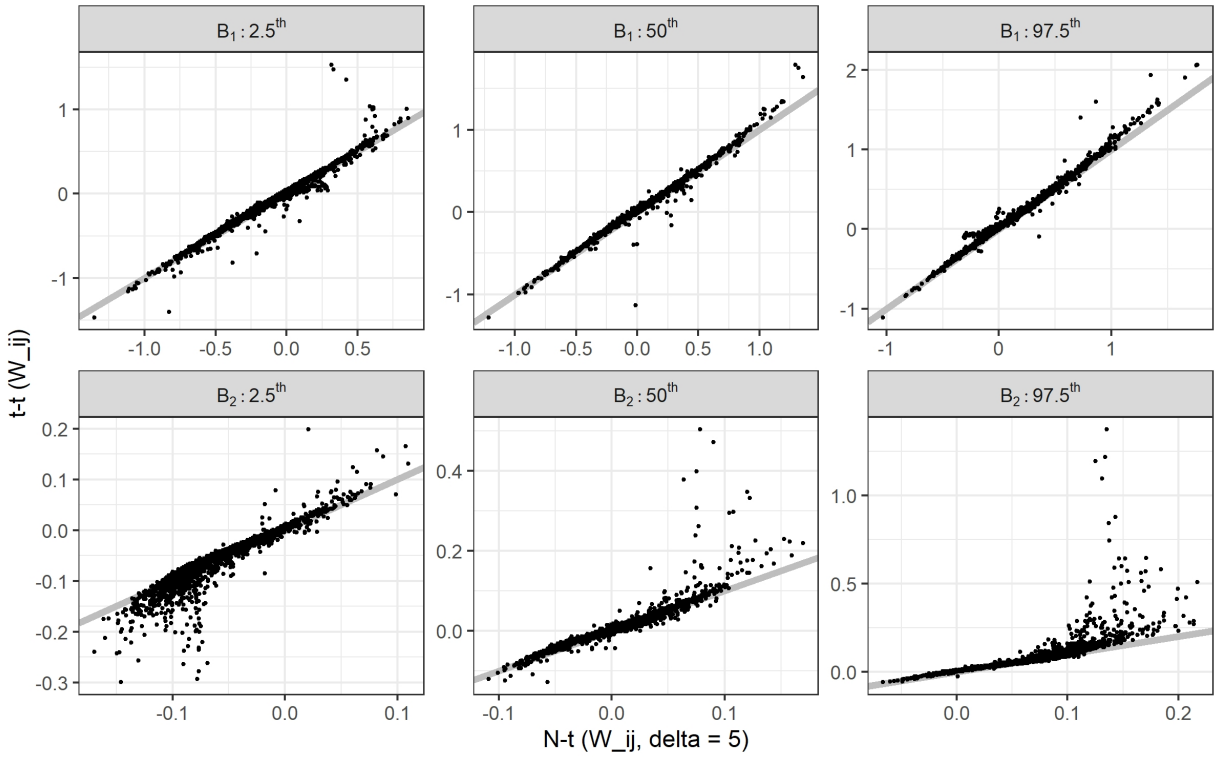


Figure 12: Scatter-plots of posterior quantiles (2.5th: left panel, 50th: mid, 97.5th: right) for $B_{1i}$ (upper panel) and $B_{2i}$ (lower panel) based on the learning data-set. x-axis is the $N-t$ $(W_{ij}, \delta = 5)$ model, y-axis the $t-t$ $(W_{ij})$. Gray lines are $x = y$ lines.

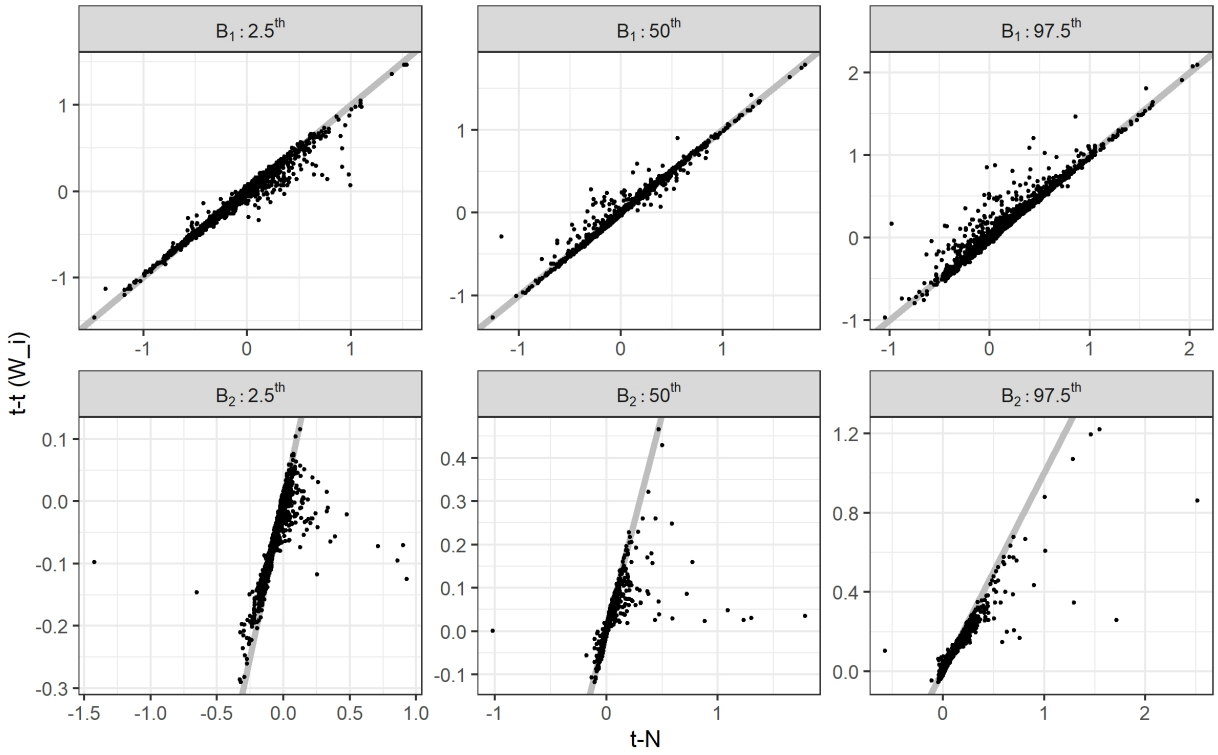


Figure 13: Scatter-plots of posterior quantiles (2.5th: left panel, 50th: mid, 97.5th: right) for $B_{1i}$ (upper panel) and $B_{2i}$ (lower panel) based on the learning data-set. x-axis is the $t - N$ model, y-axis the $t - t$ ($W_i$). Gray lines are $x = y$ lines.

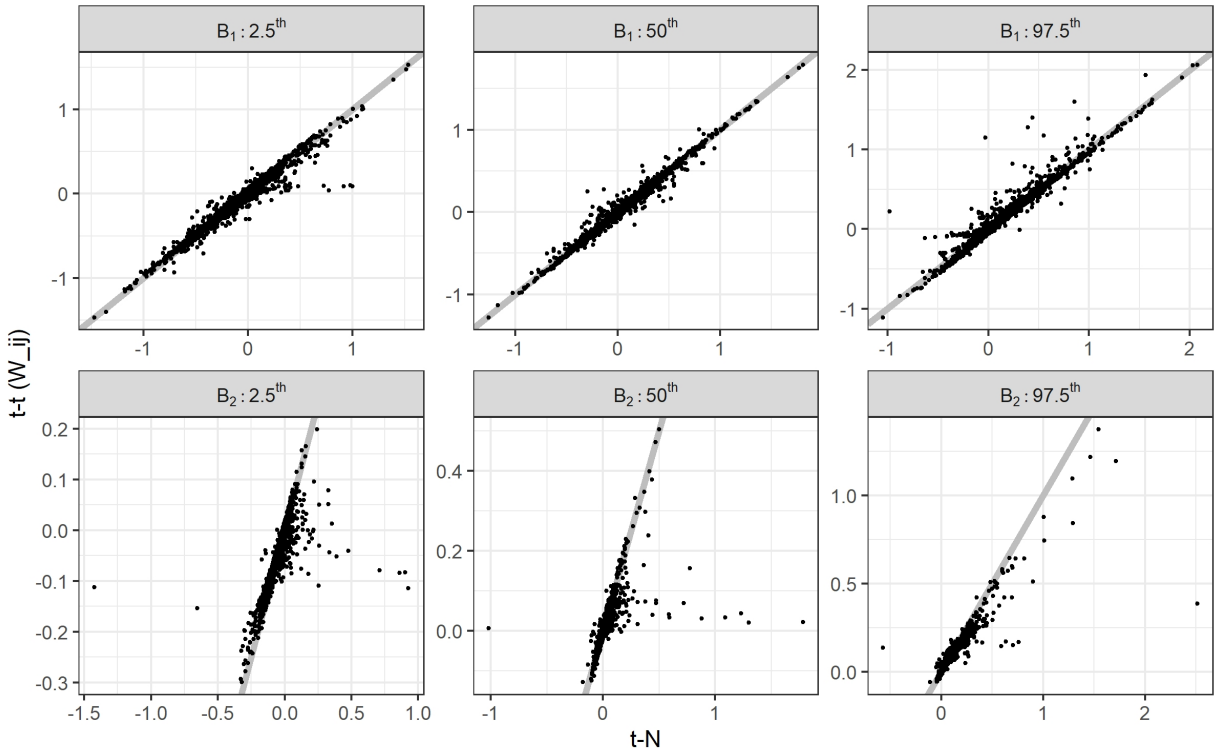


Figure 14: Scatter-plots of posterior quantiles (2.5th: left panel, 50th: mid, 97.5th: right) for $B_{1i}$ (upper panel) and $B_{2i}$ (lower panel) based on the learning data-set. x-axis is the $t - N$ model, y-axis the $t - t$ ($W_{ij}$). Gray lines are $x = y$ lines.

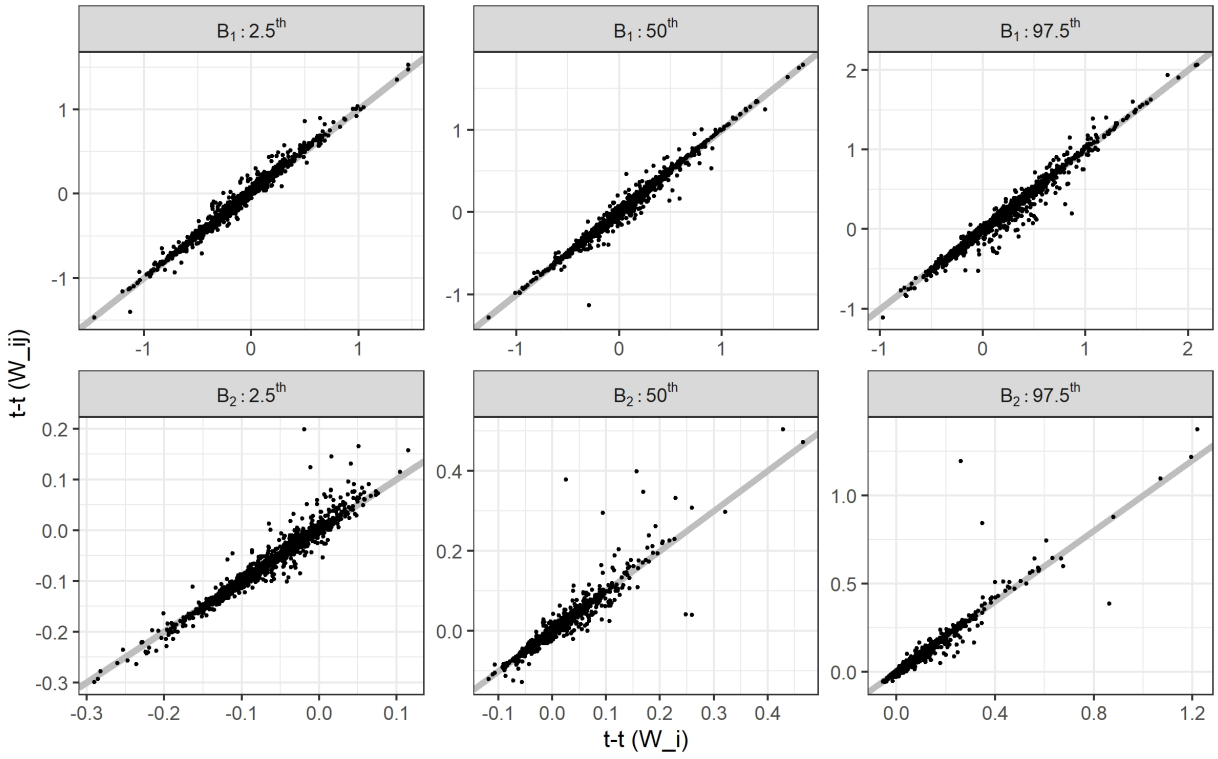


Figure 15: Scatter-plots of posterior quantiles (2.5th: left panel, 50th: mid, 97.5th: right) for $B_{1i}$ (upper panel) and $B_{2i}$ (lower panel) based on the learning data-set. x-axis is the $t-t$ $(W_i)$ model, y-axis the $t-t$ $(W_{ij})$. Gray lines are $x = y$ lines.

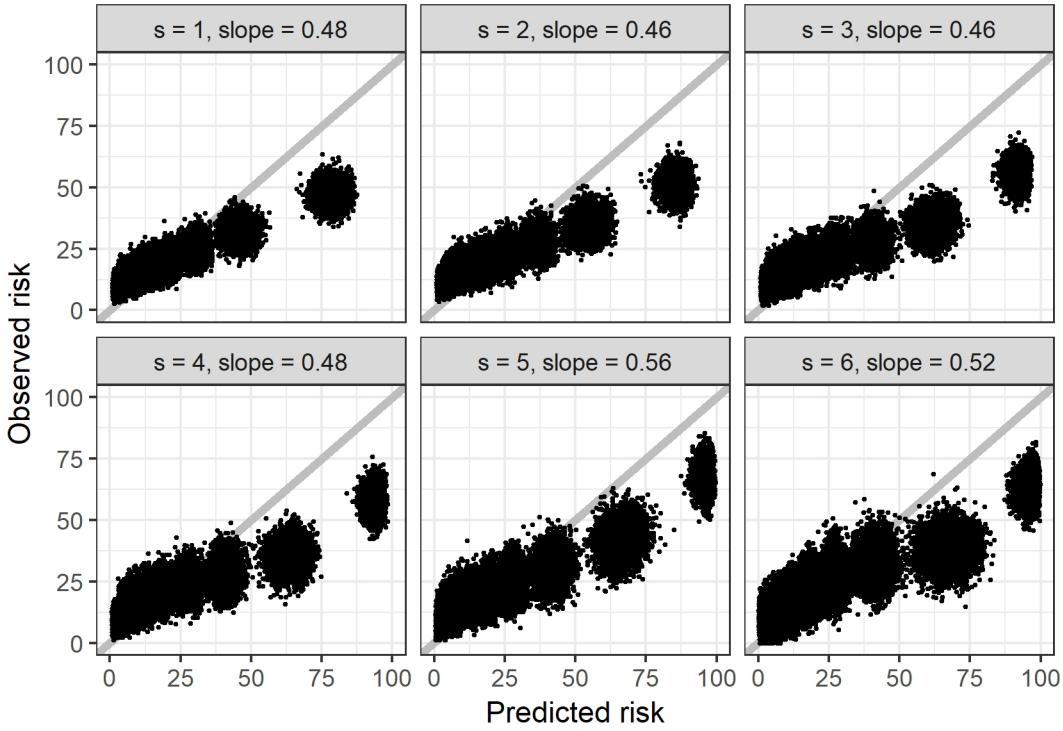


Figure 16: MCMC samples of the calibration plots based on the $N - N$ model across the landmark time-points for the internal validation. Mean predicted risks and observed risks (Kaplan-Meier) are displayed for each subgroups defined by deciles of prediction. Slope estimate is based on a simple linear regression fitted to the predicted and observed risk.

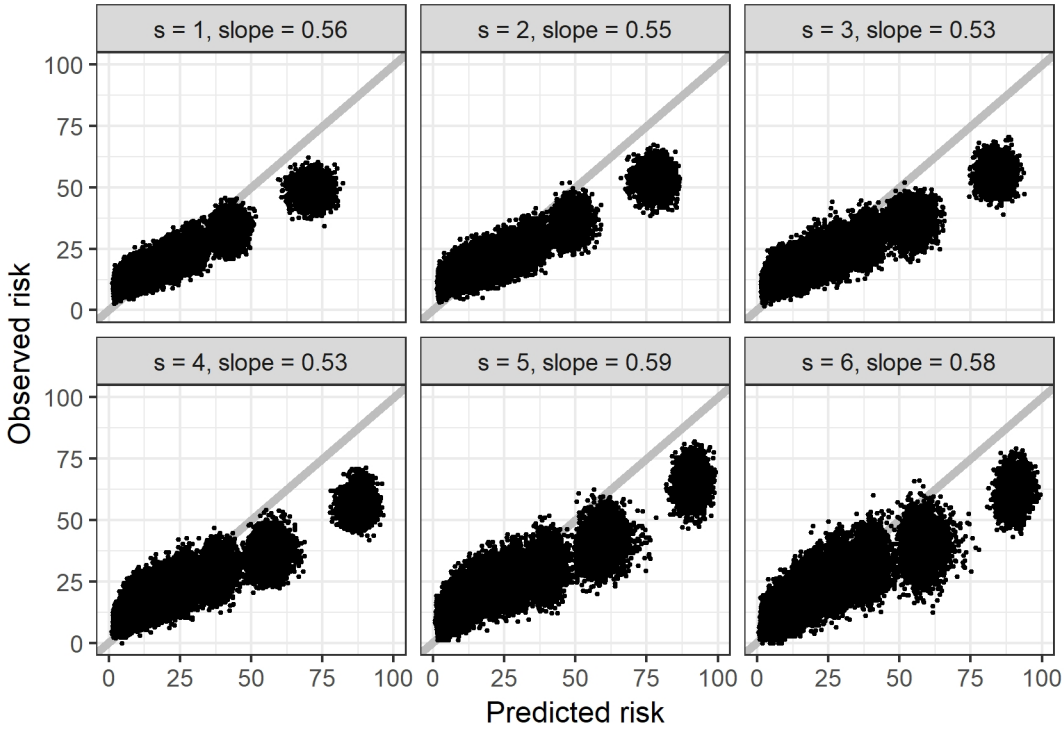


Figure 17: MCMC samples of the calibration plots based on the $N - t$ ($W_{ij}$) model across the landmark time-points for the internal validation. Mean predicted risks and observed risks (Kaplan-Meier) are displayed for each subgroups defined by deciles of prediction. Slope estimate is based on a simple linear regression fitted to the predicted and observed risk.

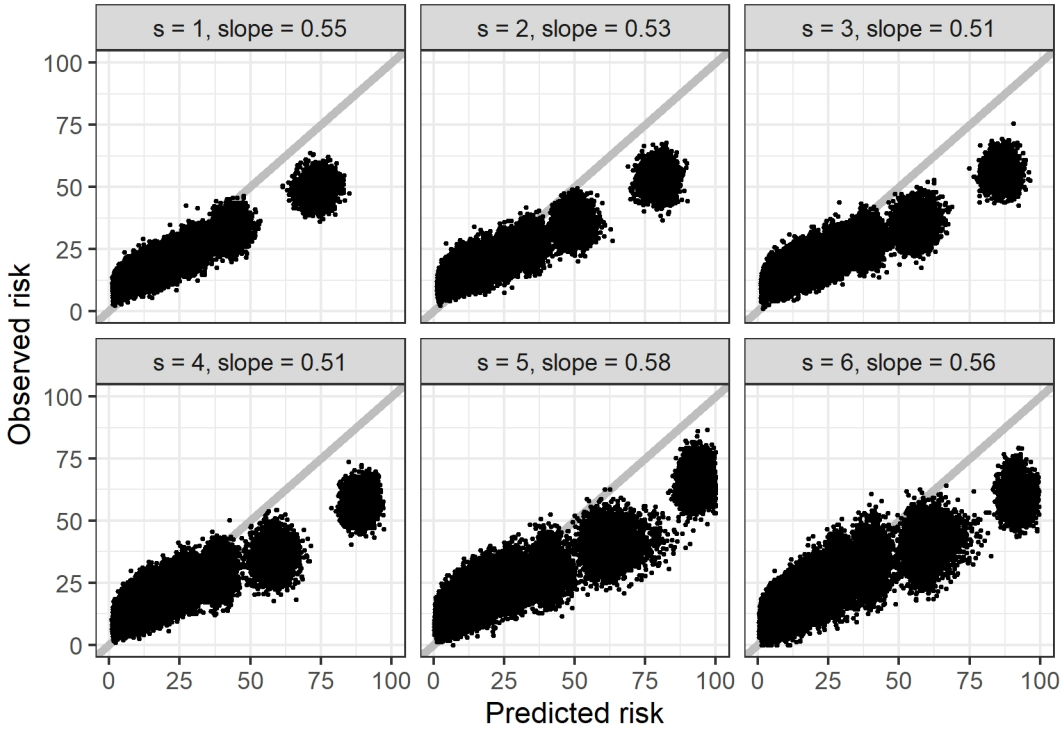


Figure 18: MCMC samples of the calibration plots based on the $N-t$ $(W_{ij}, \delta = 5)$ model across the landmark time-points for the internal validation. Mean predicted risks and observed risks (Kaplan-Meier) are displayed for each subgroups defined by deciles of prediction. Slope estimate is based on a simple linear regression fitted to the predicted and observed risk.

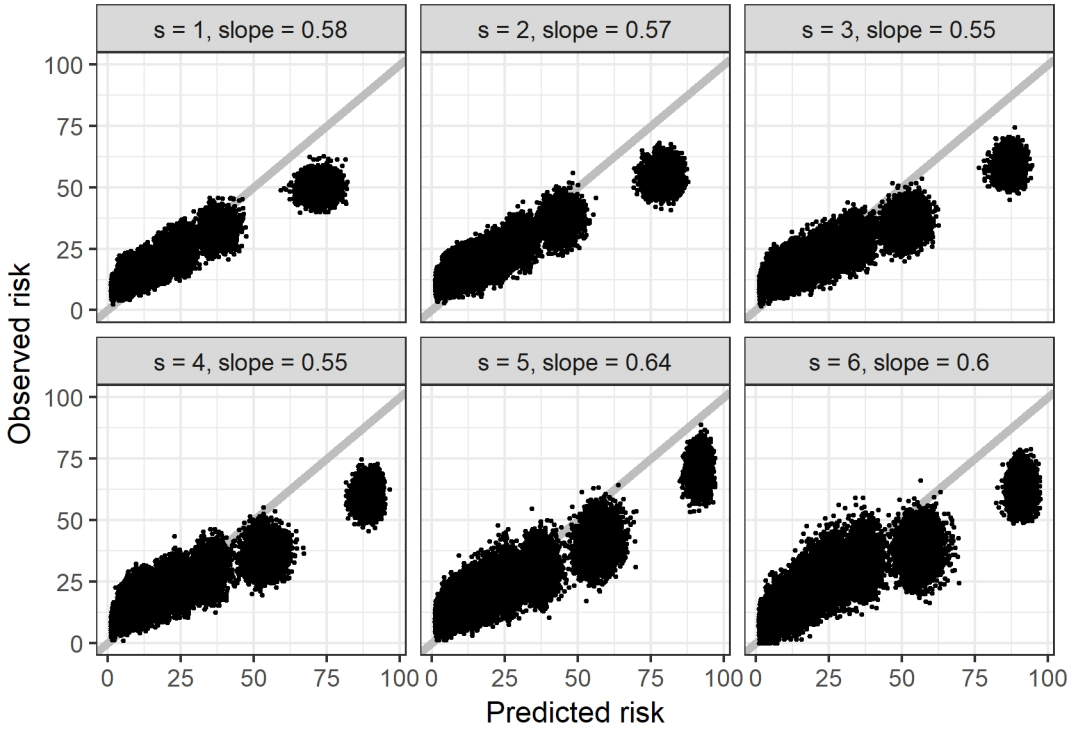


Figure 19: MCMC samples of the calibration plots based on the $t - N$ model across the landmark time-points for the internal validation. Mean predicted risks and observed risks (Kaplan-Meier) are displayed for each subgroups defined by deciles of prediction. Slope estimate is based on a simple linear regression fitted to the predicted and observed risk.

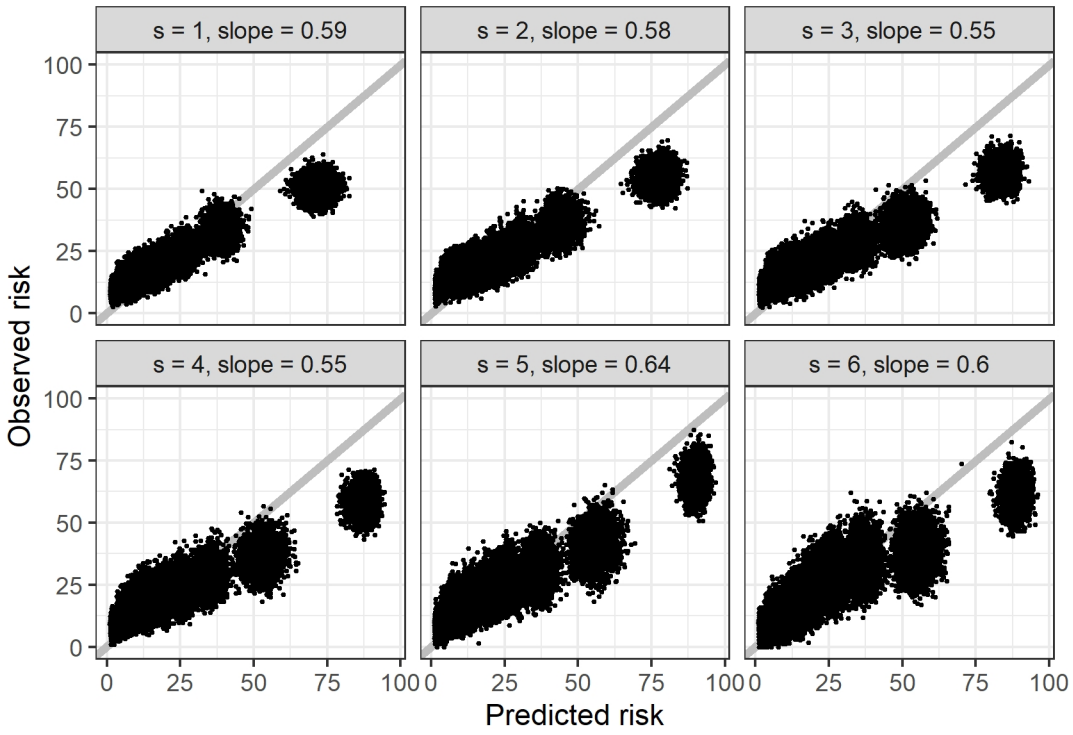


Figure 20: MCMC samples of the calibration plots based on the $t - t$ ($W_i$) model across the landmark time-points for the internal validation. Mean predicted risks and observed risks (Kaplan-Meier) are displayed for each subgroups defined by deciles of prediction. Slope estimate is based on a simple linear regression fitted to the predicted and observed risk.

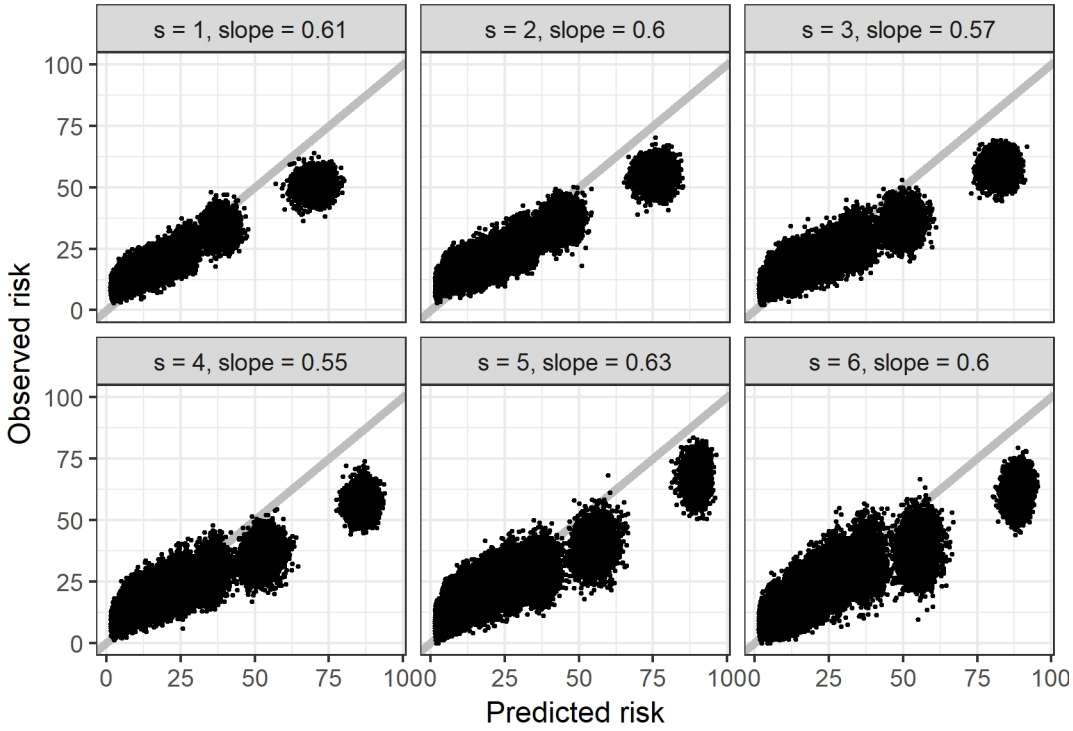


Figure 21: MCMC samples of the calibration plots based on the $t - t$ ($W_{ij}$) model across the landmark time-points for the internal validation. Mean predicted risks and observed risks (Kaplan-Meier) are displayed for each subgroups defined by deciles of prediction. Slope estimate is based on a simple linear regression fitted to the predicted and observed risk.

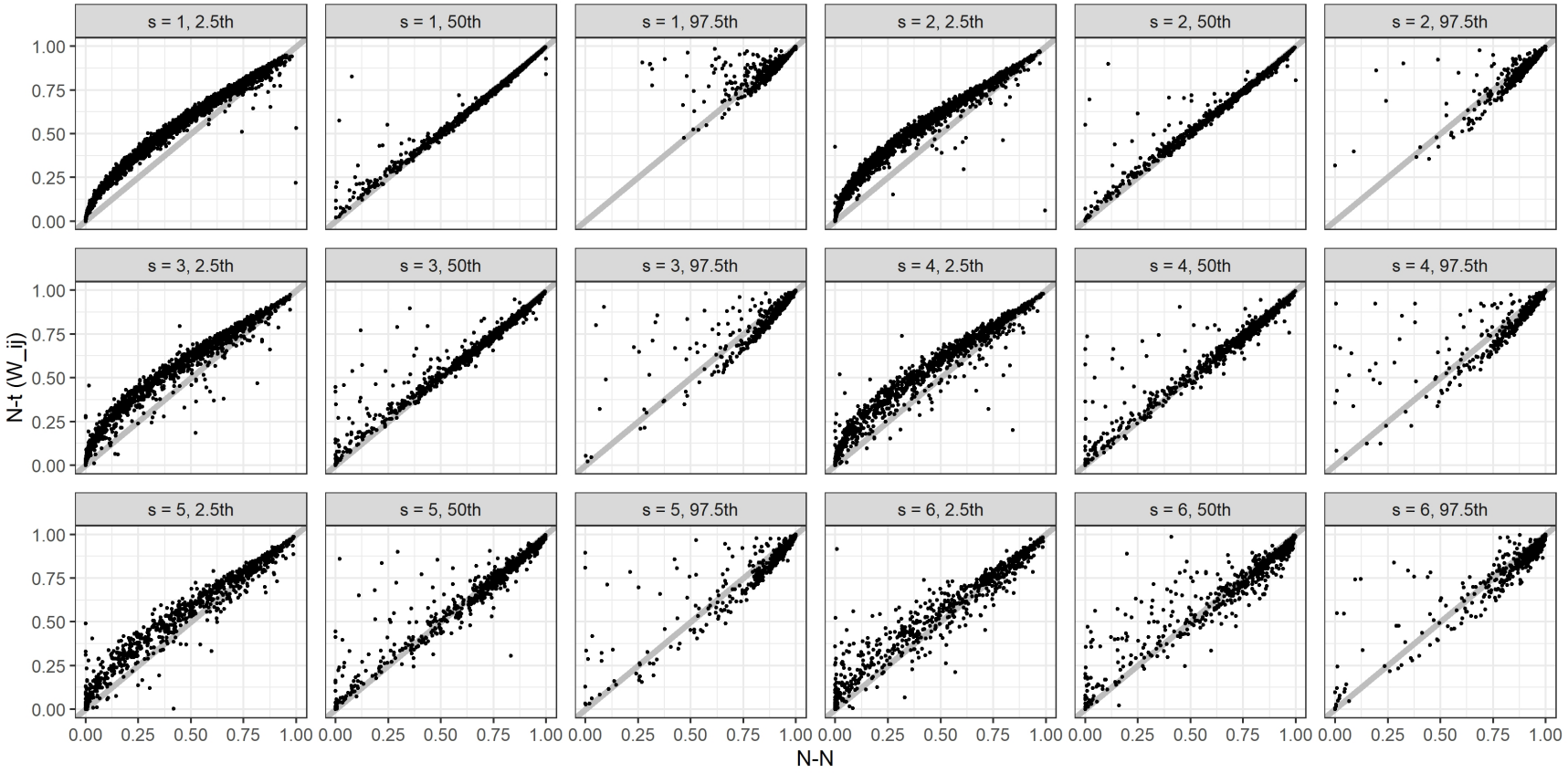


Figure 22: Scatter-plots of the 2.5th, 50th and 97.5th quantiles of the dynamic predictions across landmark time-points ($s = 1, 2, 3, 4, 5, 6$) for the internal validation. x-axis is the $N - N$ model, y-axis the $N - t$ ($W_{ij}$). Gray lines are $x = y$ lines.

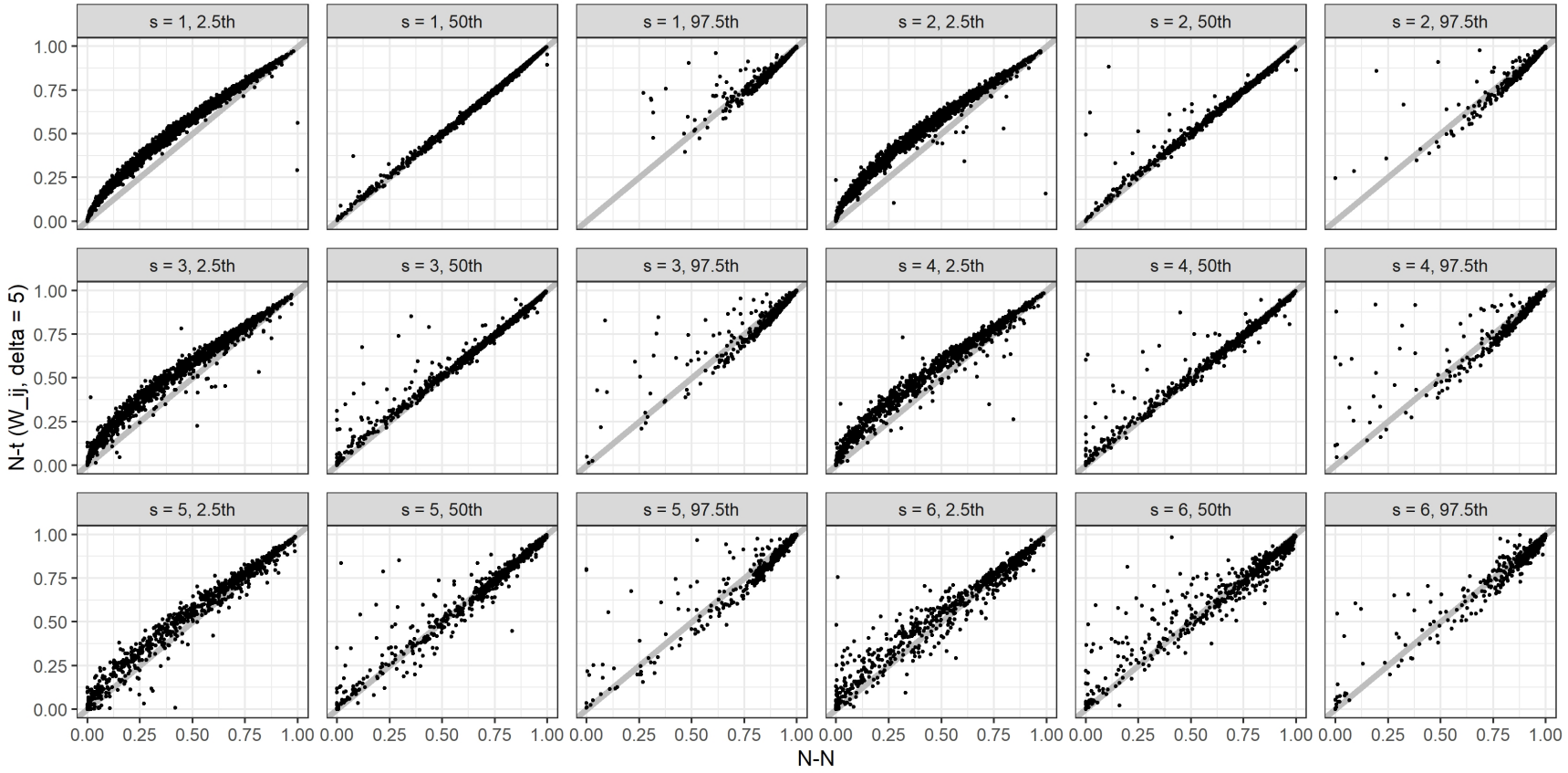


Figure 23: Scatter-plots of the 2.5th, 50th and 97.5th quantiles of the dynamic predictions across landmark time-points ($s = 1, 2, 3, 4, 5, 6$) for the internal validation. x-axis is the $N - N$ model, y-axis the $N - t$ ($W_{ij}, \delta = 5$). Gray lines are $x = y$ lines.

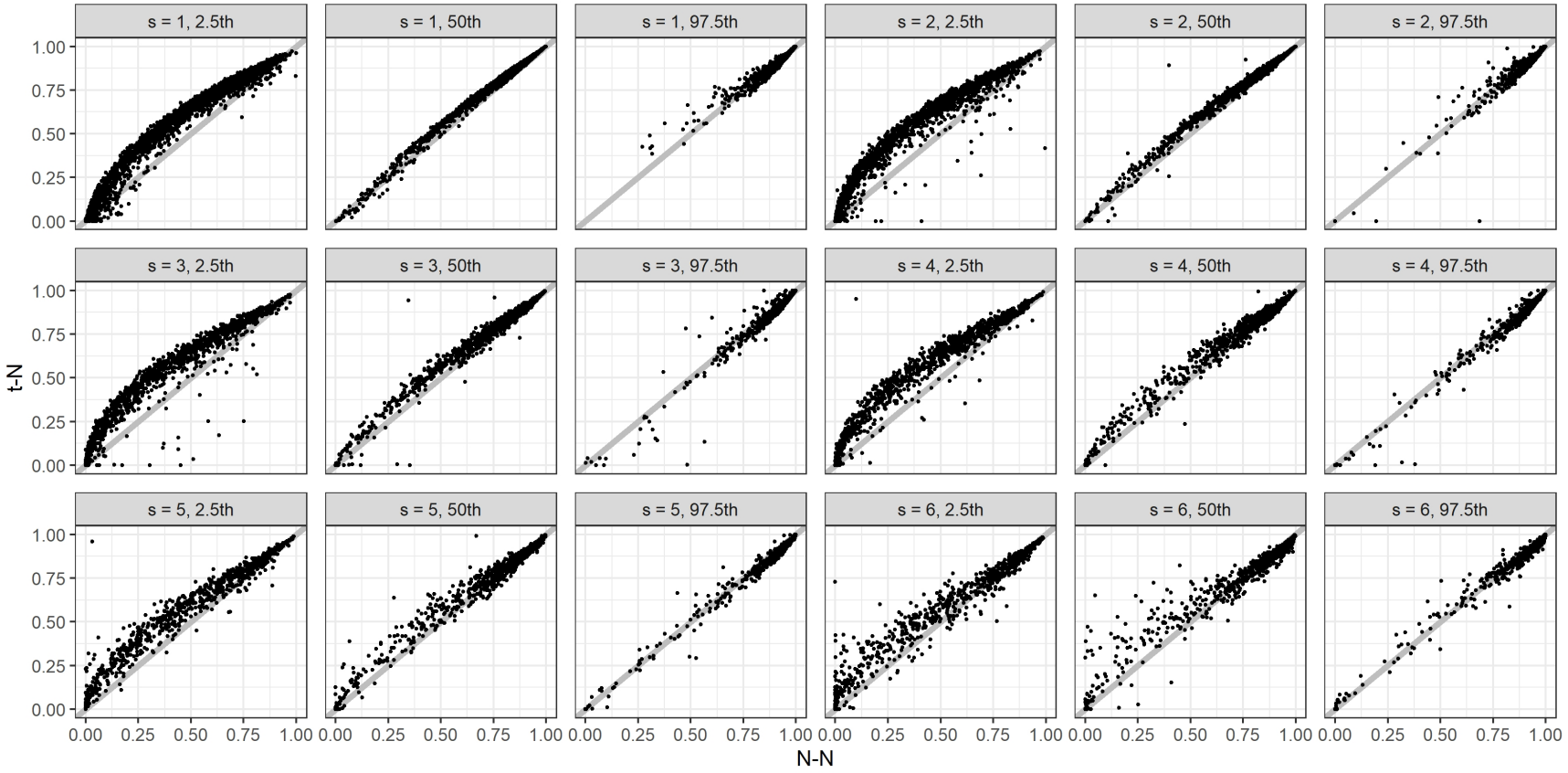


Figure 24: Scatter-plots of the 2.5th, 50th and 97.5th quantiles of the dynamic predictions across landmark time-points ($s = 1, 2, 3, 4, 5, 6$) for the internal validation. x-axis is the $N - N$ model, y-axis the $N - t$. Gray lines are $x = y$ lines.

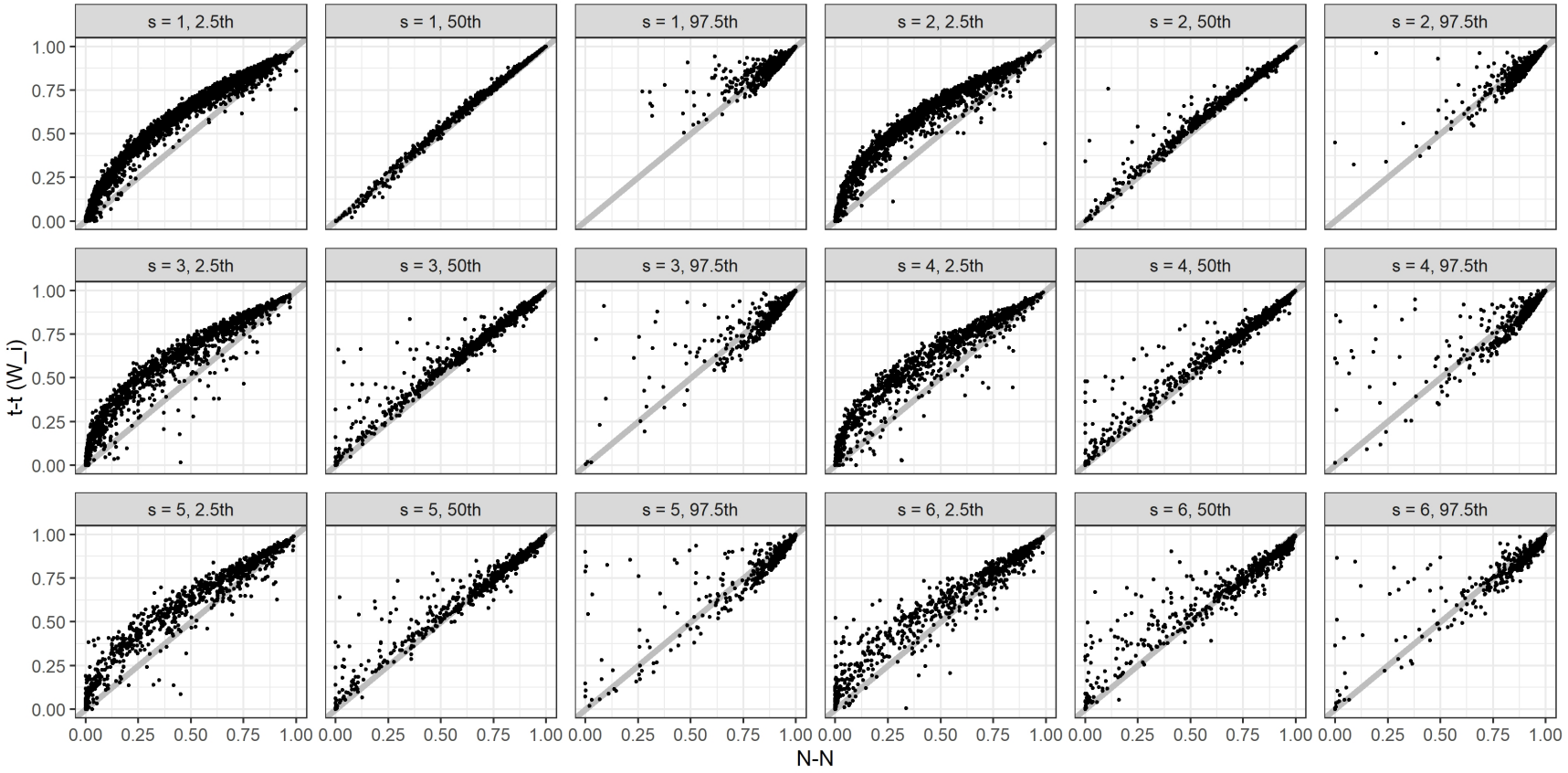


Figure 25: Scatter-plots of the 2.5th, 50th and 97.5th quantiles of the dynamic predictions across landmark time-points ($s = 1, 2, 3, 4, 5, 6$) for the internal validation. x-axis is the $N - N$ model, y-axis the $t - t$ ($W_i$). Gray lines are $x = y$ lines.

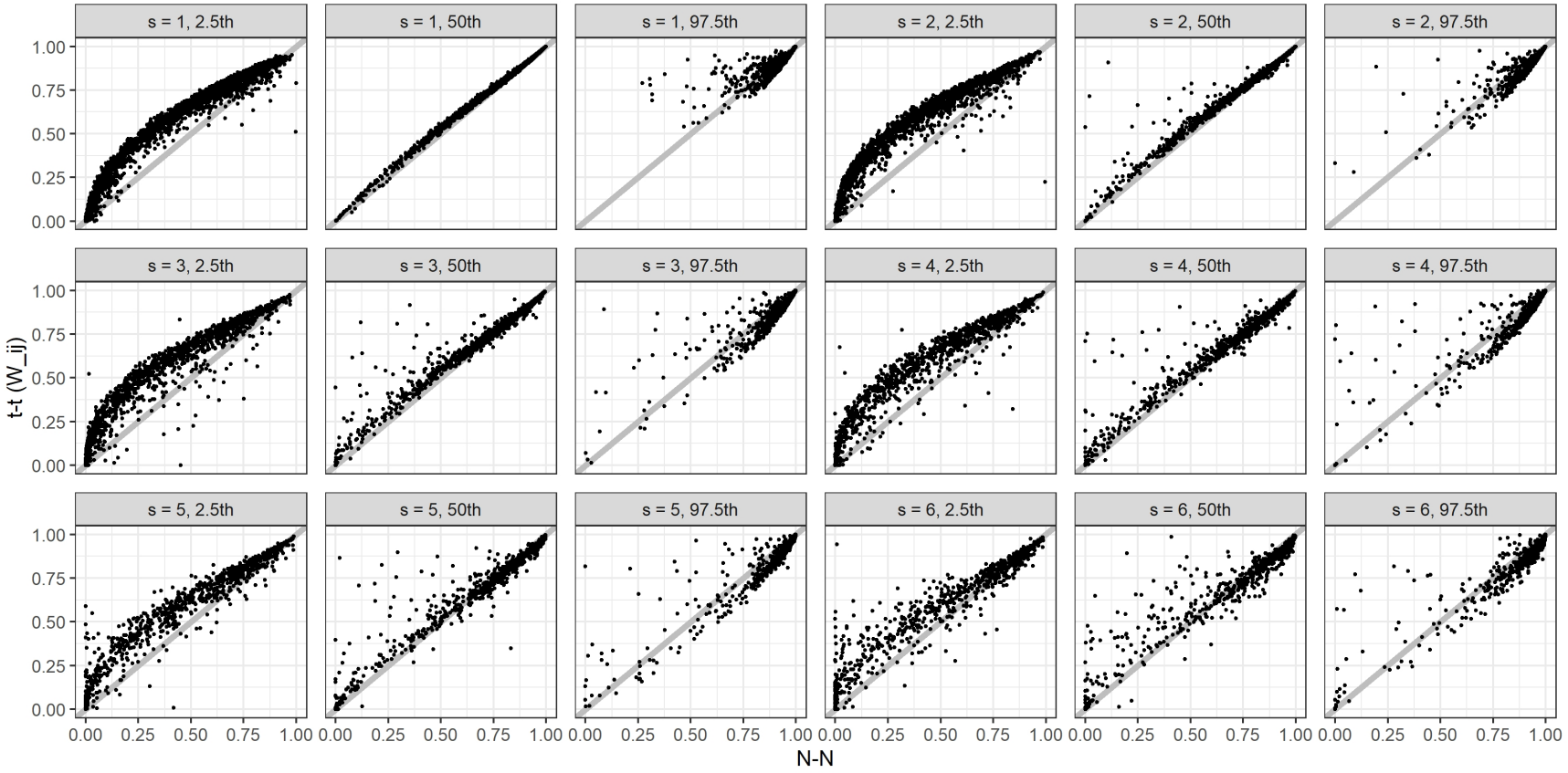


Figure 26: Scatter-plots of the 2.5th, 50th and 97.5th quantiles of the dynamic predictions across landmark time-points ($s = 1, 2, 3, 4, 5, 6$) for the internal validation. x-axis is the $N - N$ model, y-axis the $t - t$ ($W_{ij}$). Gray lines are $x = y$ lines.

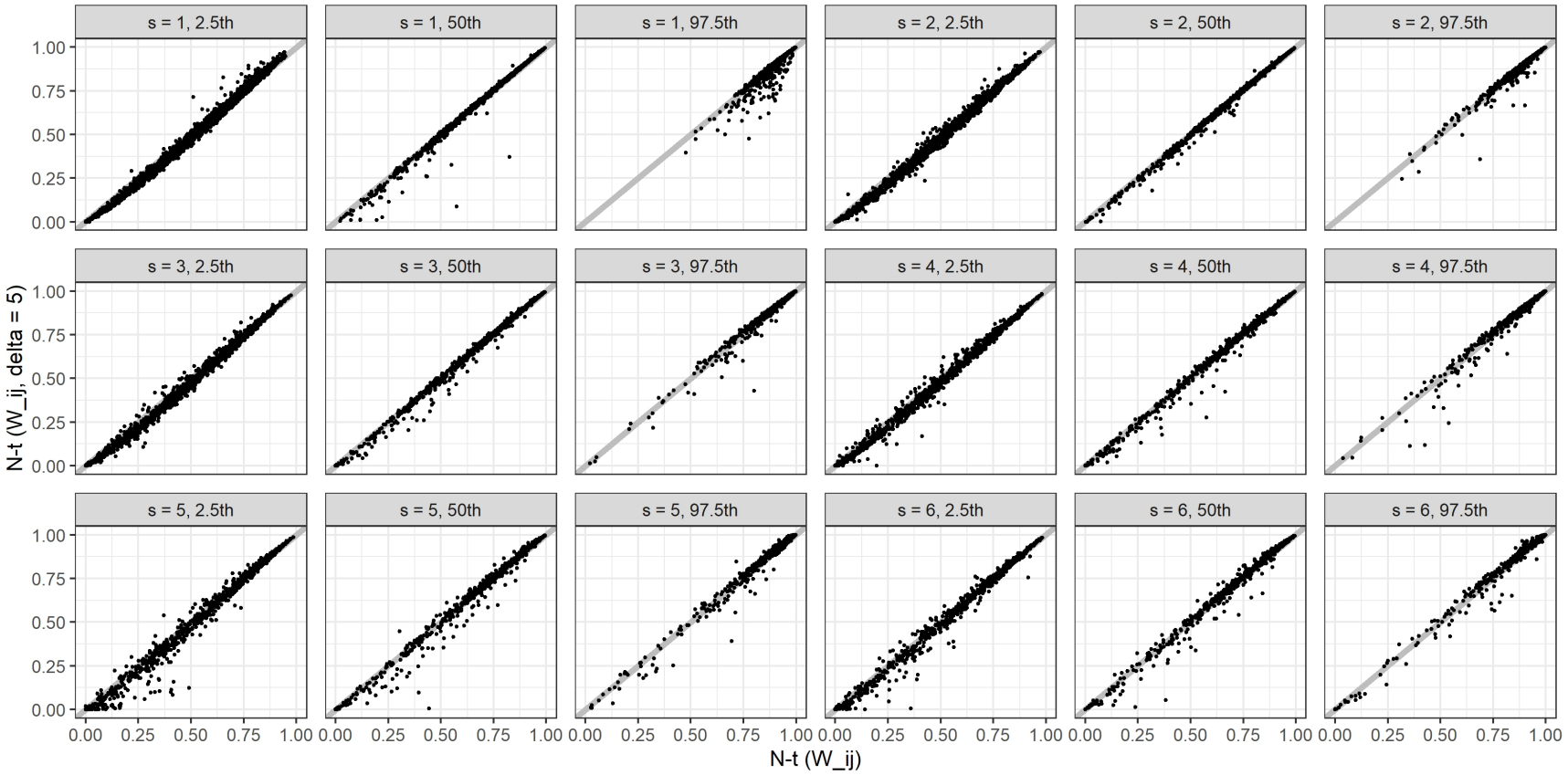


Figure 27: Scatter-plots of the 2.5th, 50th and 97.5th quantiles of the dynamic predictions across landmark time-points ($s = 1, 2, 3, 4, 5, 6$) for the internal validation. x-axis is the $N - t$ $(W_{ij})$ model, y-axis the $N - t$ $(W_{ij}, \delta = 5)$. Gray lines are $x = y$ lines.

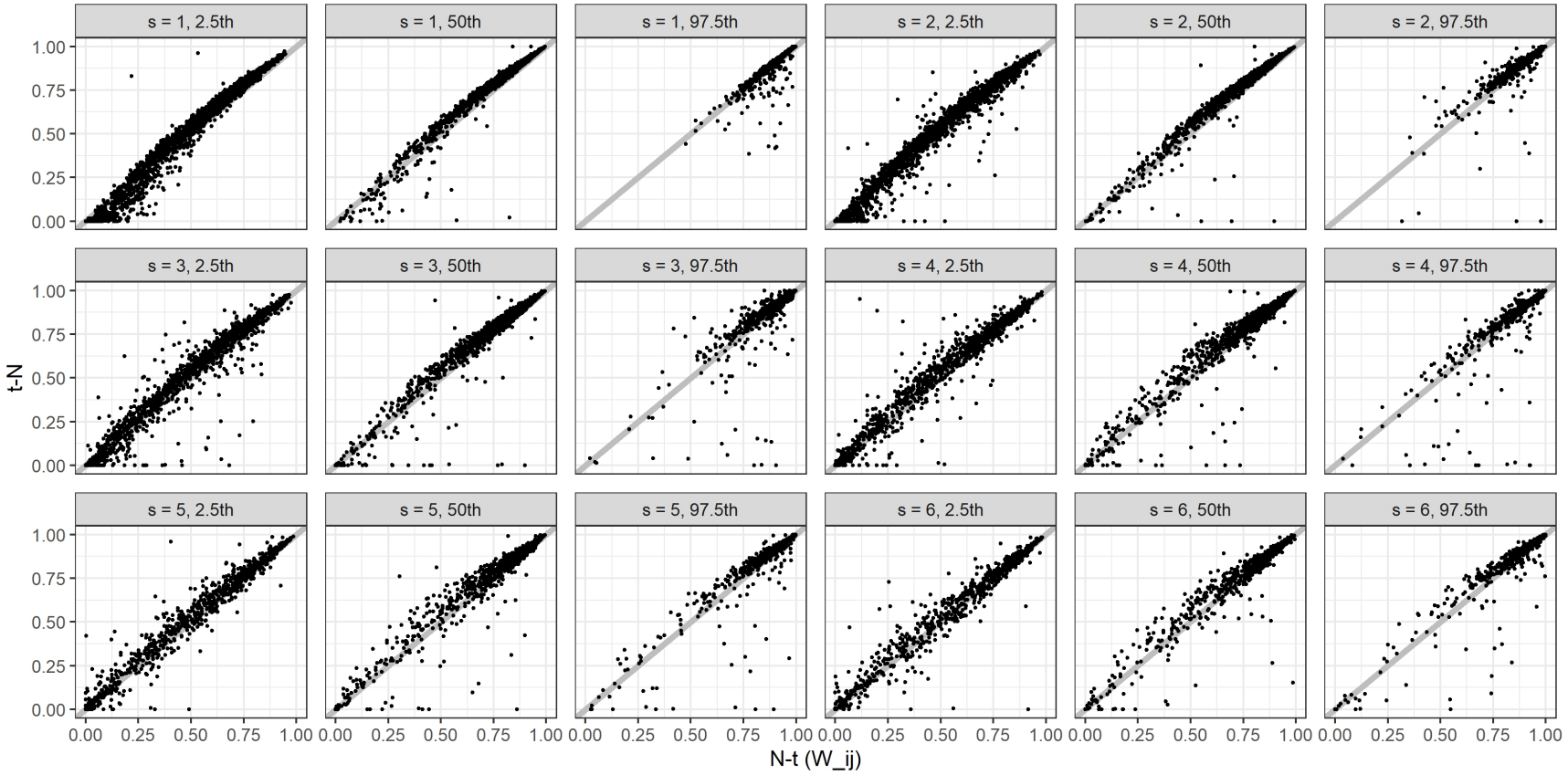


Figure 28: Scatter-plots of the 2.5th, 50th and 97.5th quantiles of the dynamic predictions across landmark time-points ($s = 1, 2, 3, 4, 5, 6$) for the internal validation. x-axis is the $N - t$ ($W_{ij}$) model, y-axis the $t - N$. Gray lines are $x = y$ lines.

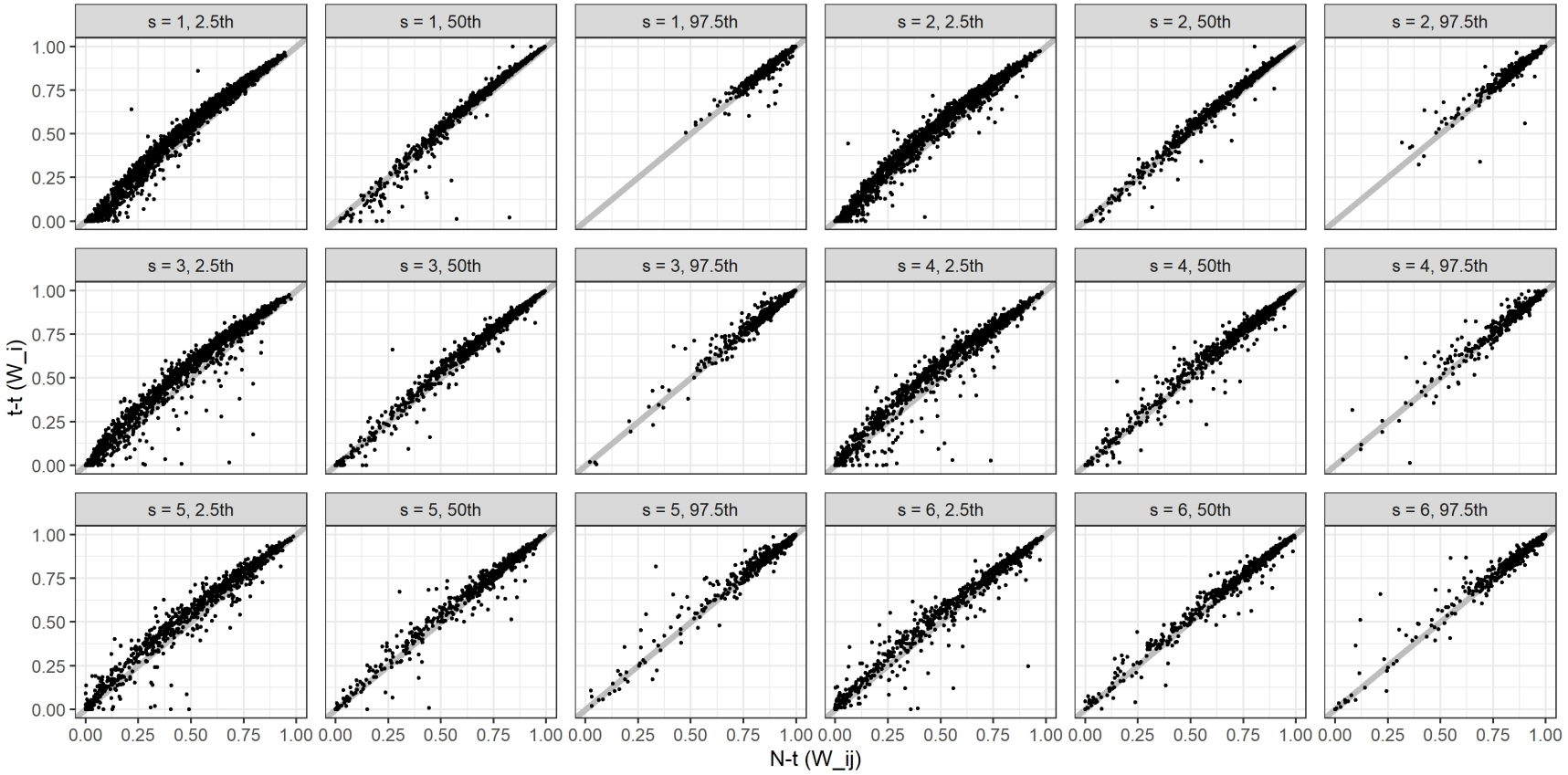


Figure 29: Scatter-plots of the 2.5th, 50th and 97.5th quantiles of the dynamic predictions across landmark time-points ($s = 1, 2, 3, 4, 5, 6$) for the internal validation. x-axis is the $N - t$ ($W_{ij}$) model, y-axis the $t - t$ ($W_i$). Gray lines are $x = y$ lines.

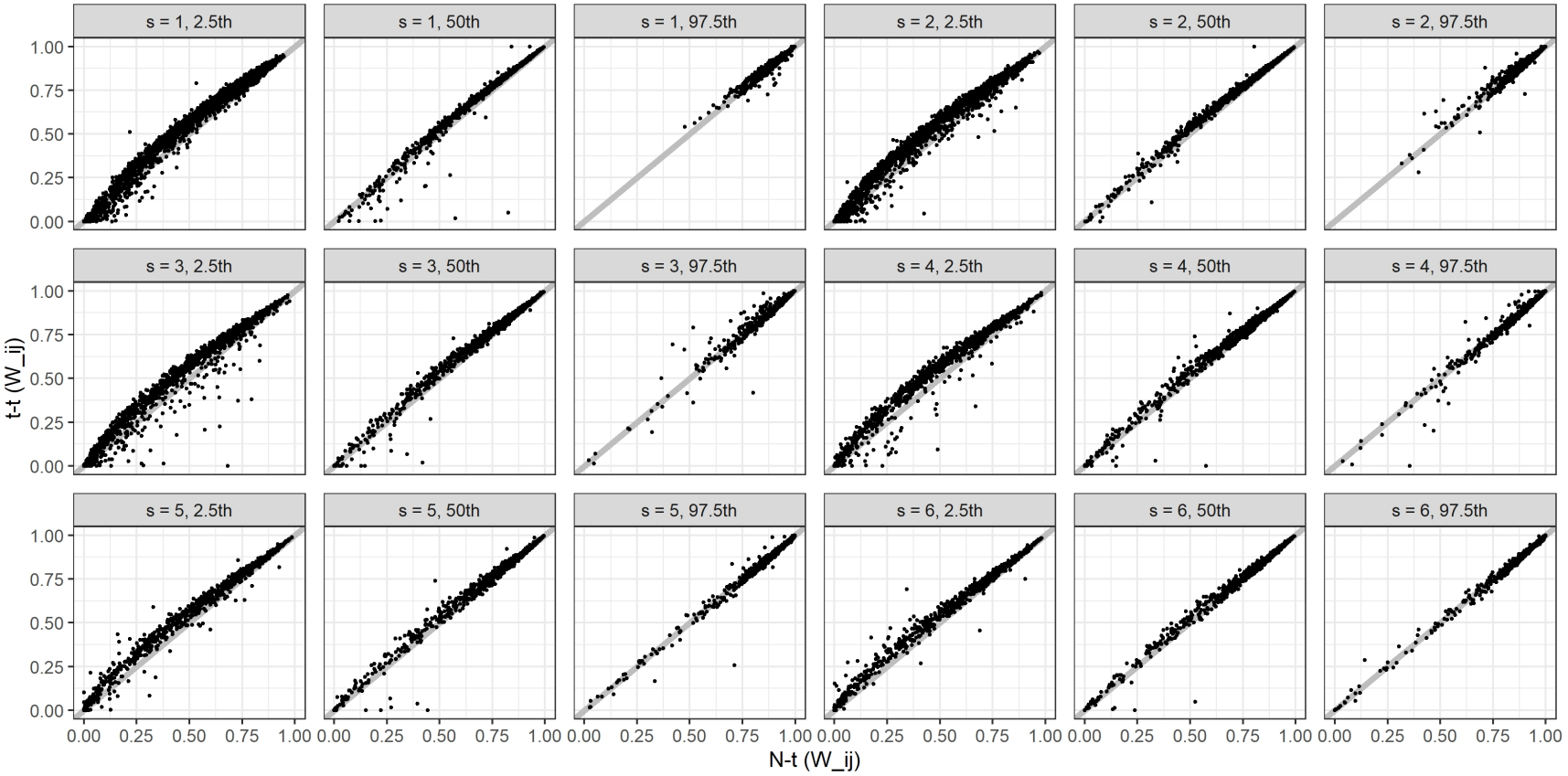


Figure 30: Scatter-plots of the 2.5th, 50th and 97.5th quantiles of the dynamic predictions across landmark time-points ($s = 1, 2, 3, 4, 5, 6$) for the internal validation. x-axis is the $N - t$ ($W_{ij}$) model, y-axis the $t - t$ ($W_{ij}$). Gray lines are $x = y$ lines.

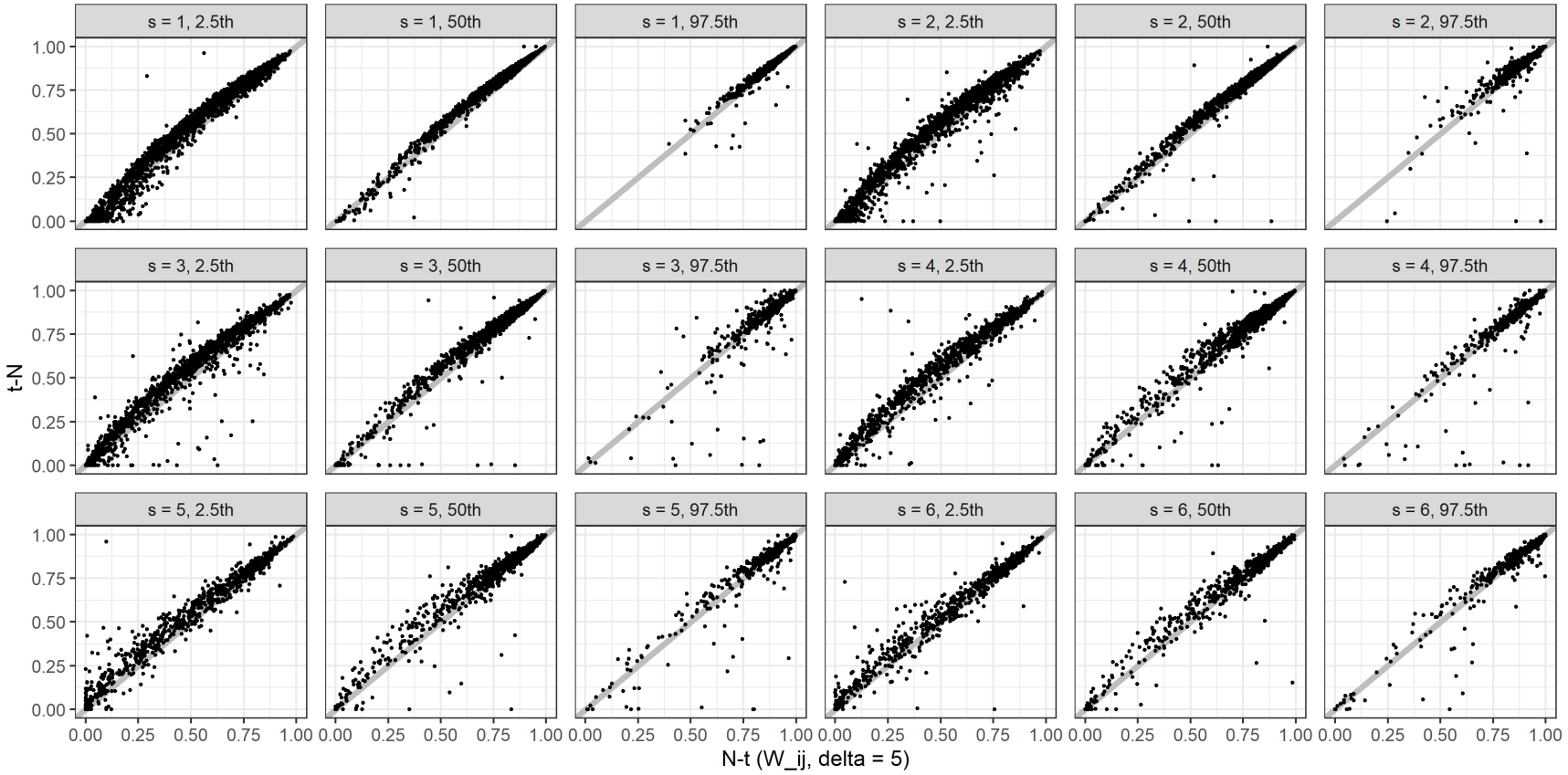


Figure 31: Scatter-plots of the 2.5th, 50th and 97.5th quantiles of the dynamic predictions across landmark time-points ($s = 1, 2, 3, 4, 5, 6$) for the internal validation. x-axis is the $N - t$ ($W_{ij}, \delta = 5$) model, y-axis the $t - N$. Gray lines are $x = y$ lines.

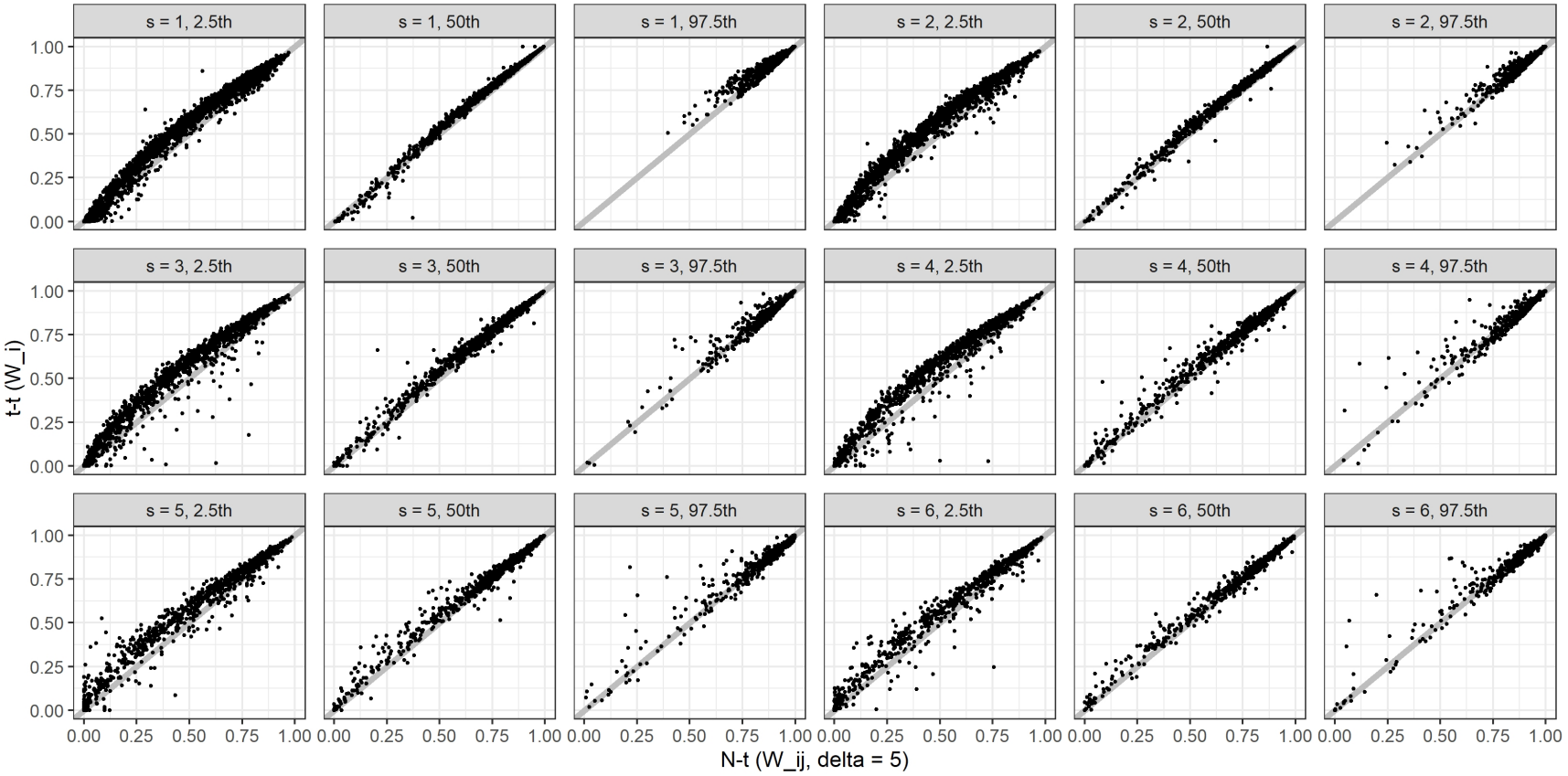


Figure 32: Scatter-plots of the 2.5th, 50th and 97.5th quantiles of the dynamic predictions across landmark time-points ($s = 1, 2, 3, 4, 5, 6$) for the internal validation. x-axis is the $N - t$ ($W_{ij}, \delta = 5$) model, y-axis the $t - t$ ($W_i$). Gray lines are $x = y$ lines.

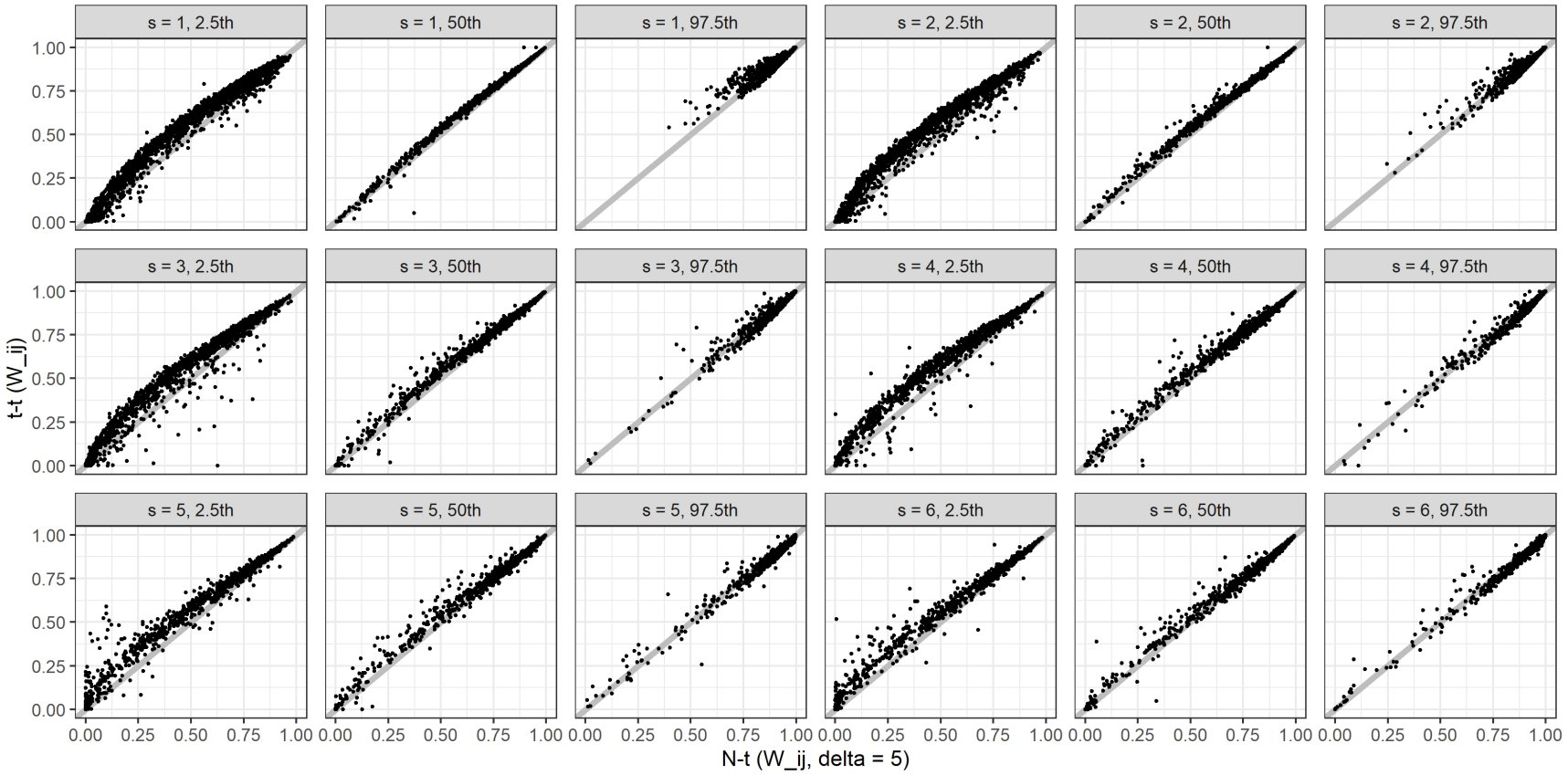


Figure 33: Scatter-plots of the 2.5th, 50th and 97.5th quantiles of the dynamic predictions across landmark time-points ($s = 1, 2, 3, 4, 5, 6$) for the internal validation. x-axis is the $N - t$ $(W_{ij}, \delta = 5)$ model, y-axis the $t - t$ $(W_{ij})$. Gray lines are $x = y$ lines.

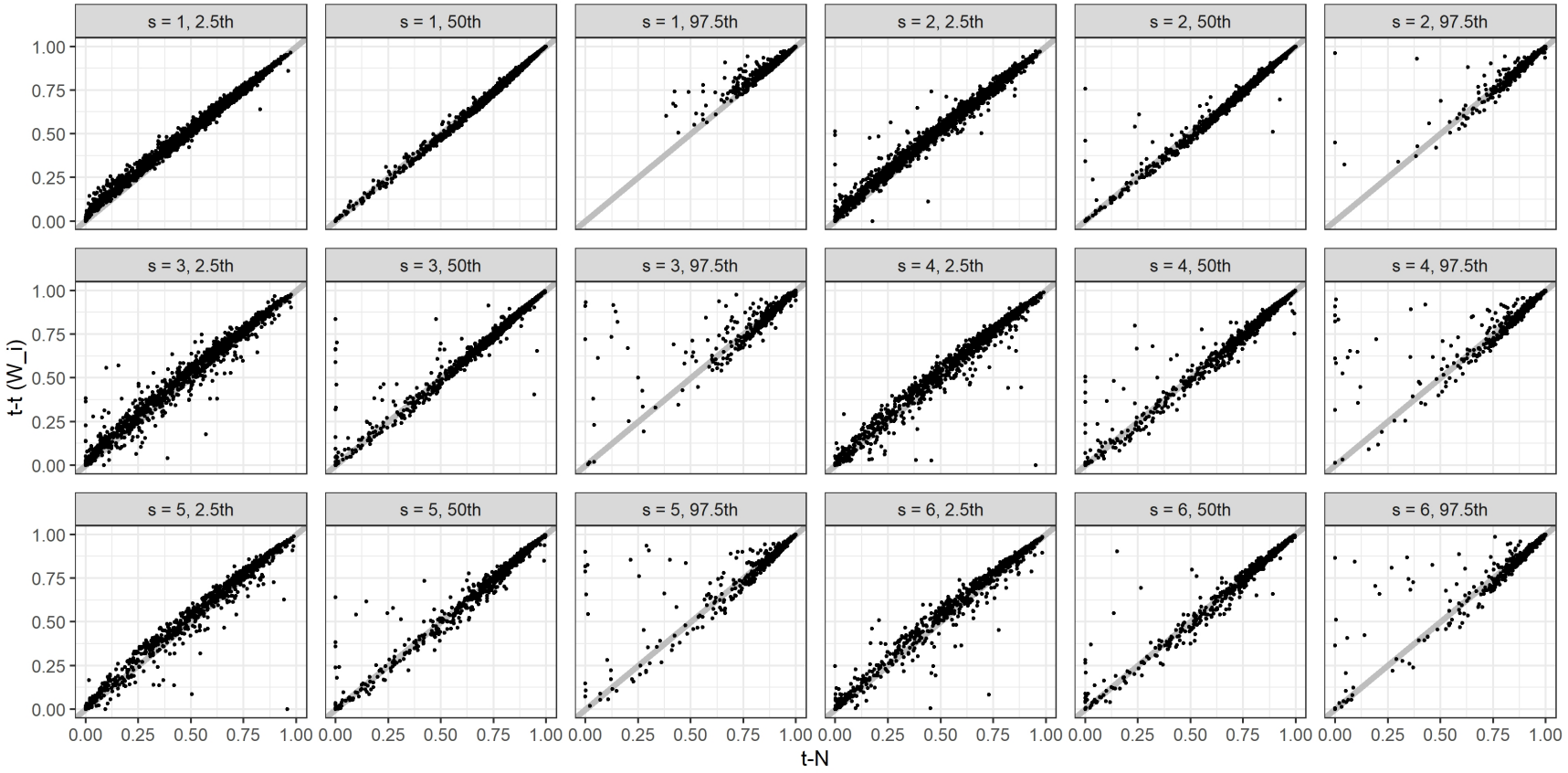


Figure 34: Scatter-plots of the 2.5th, 50th and 97.5th quantiles of the dynamic predictions across landmark time-points ($s = 1, 2, 3, 4, 5, 6$) for the internal validation. x-axis is the $t - N$ model, y-axis the $t - t$ ($W_i$). Gray lines are $x = y$ lines.

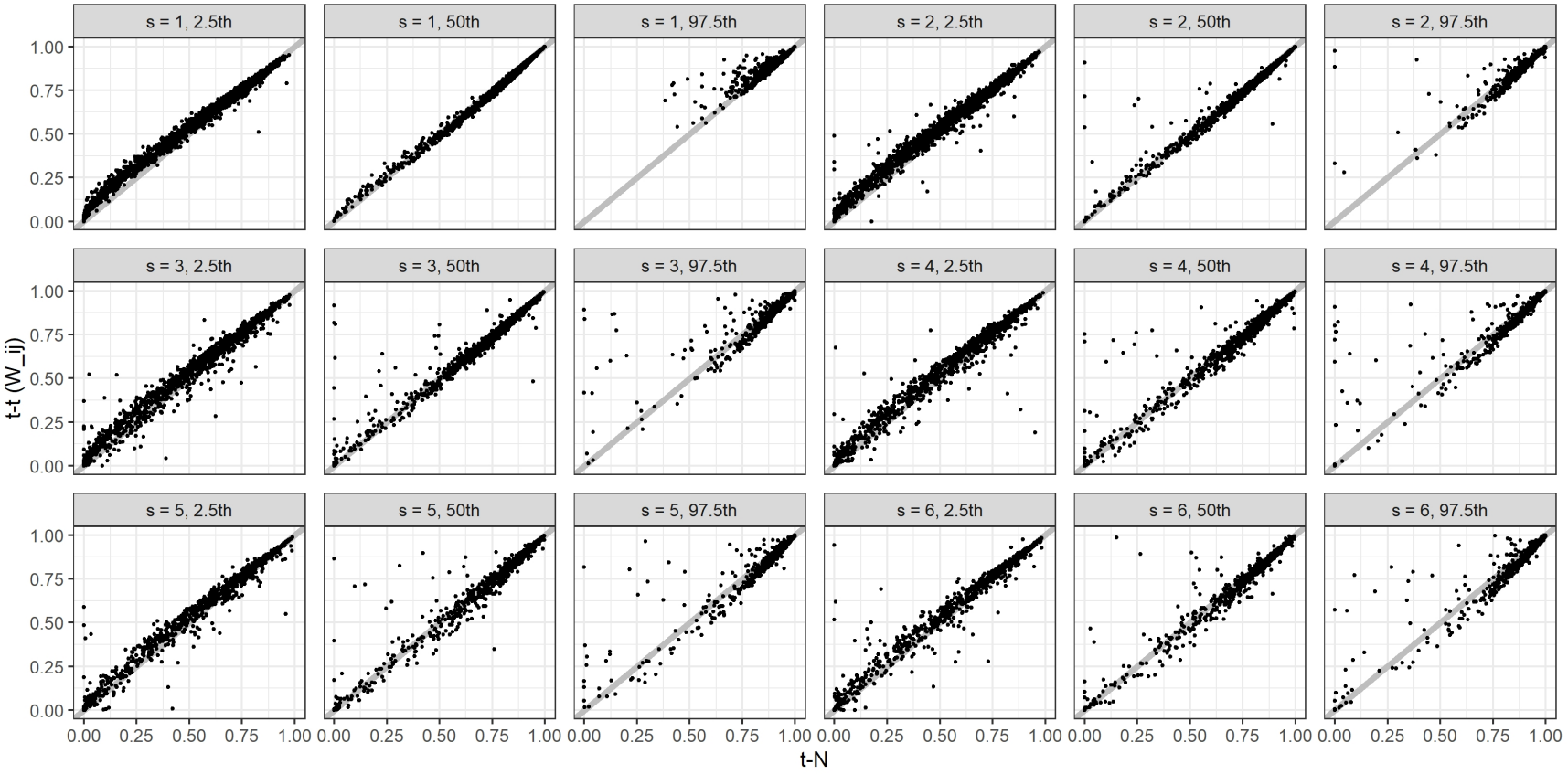


Figure 35: Scatter-plots of the 2.5th, 50th and 97.5th quantiles of the dynamic predictions across landmark time-points ($s = 1, 2, 3, 4, 5, 6$) for the internal validation. x-axis is the $t - N$ model, y-axis the $t - t$ ($W_{ij}$). Gray lines are $x = y$ lines.

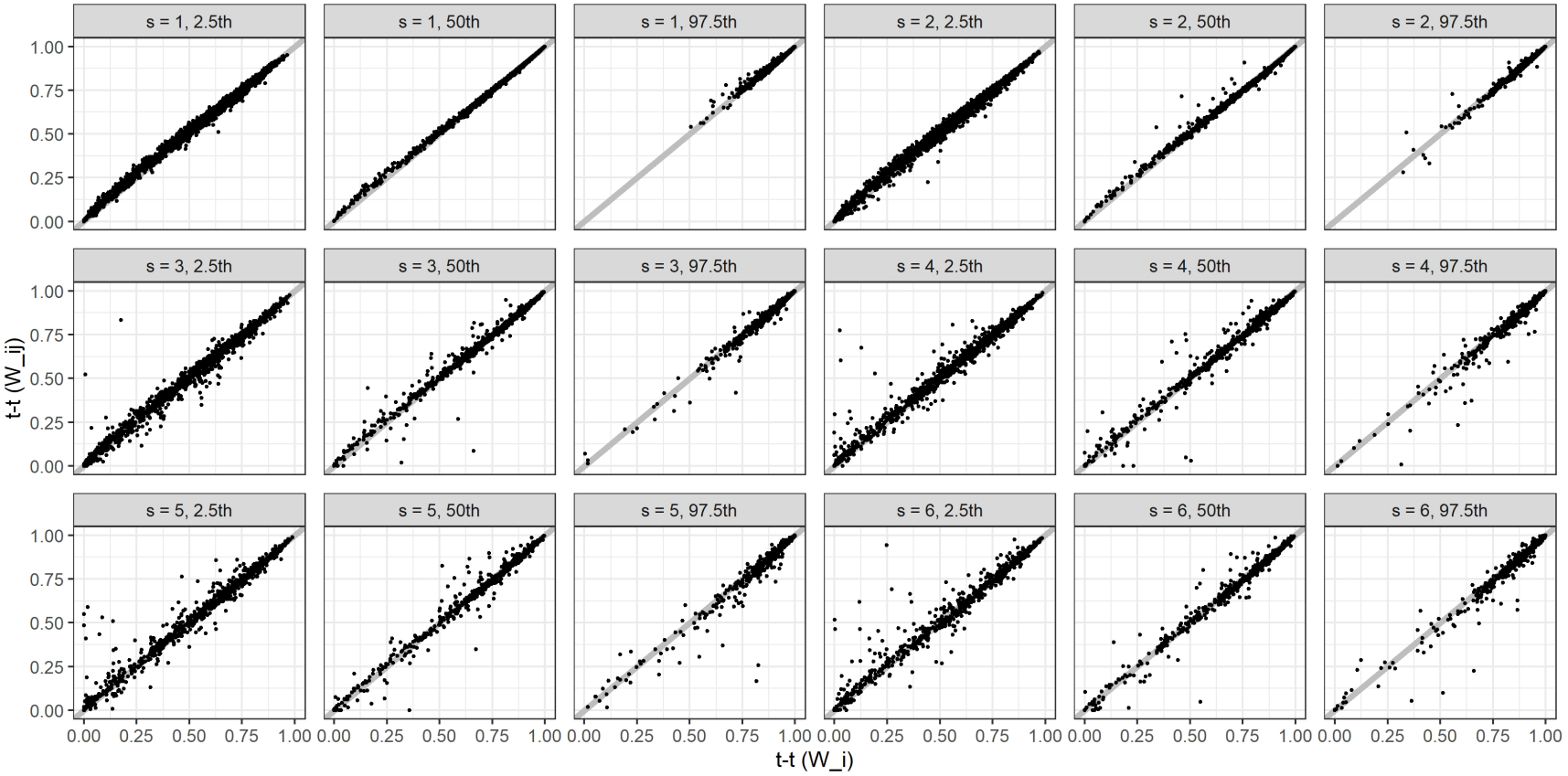


Figure 36: Scatter-plots of the 2.5th, 50th and 97.5th quantiles of the dynamic predictions across landmark time-points ($s = 1, 2, 3, 4, 5, 6$) for the internal validation. x-axis is the $t - t$ ($W_i$) model, y-axis the $t - t$ ($W_{ij}$). Gray lines are $x = y$ lines.

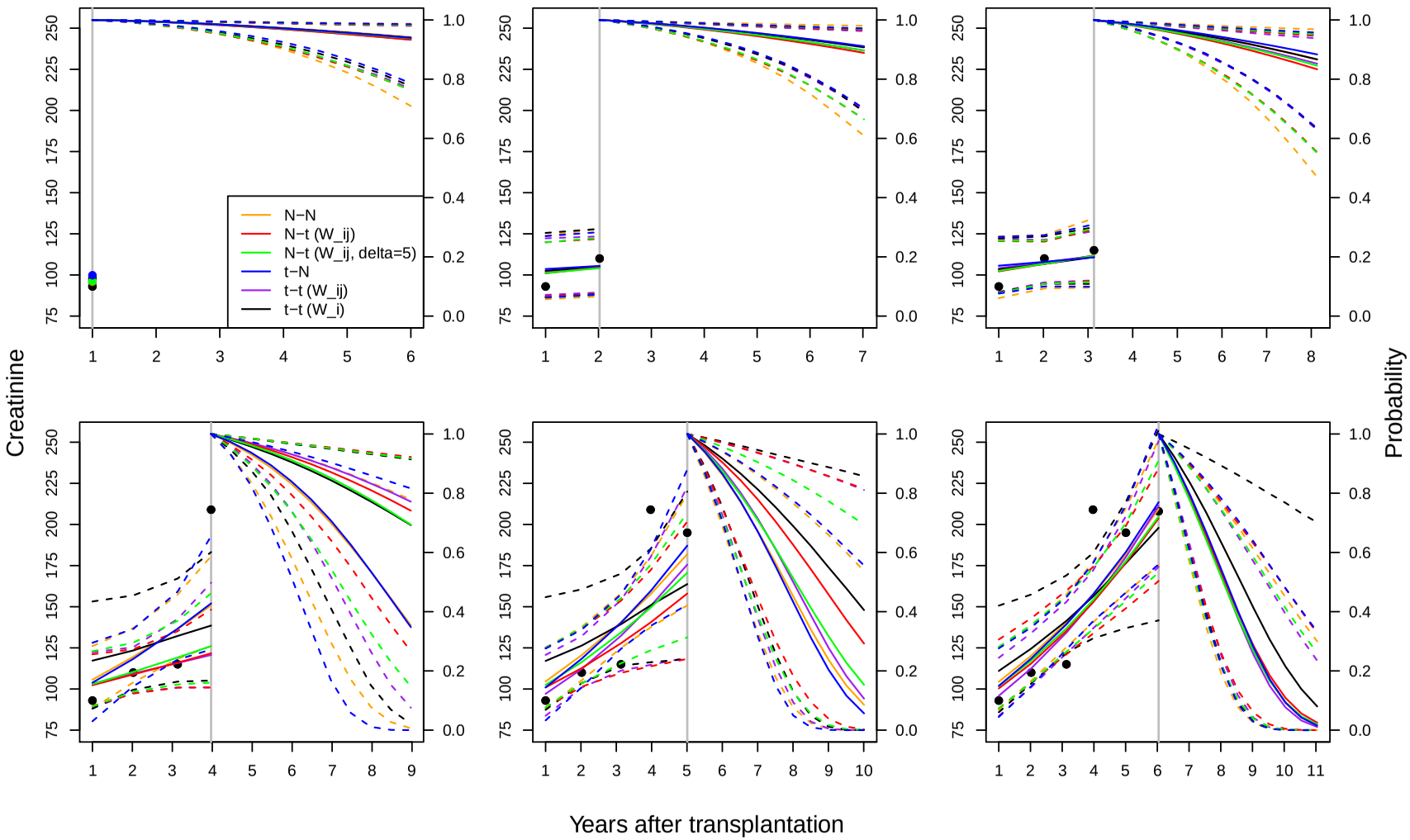


Figure 37: Dynamic predictions for the first person from the validation sample. Dots are observed data. Colours indicate different models; see the legend box in the upper-left panel. Dashed lower and upper lines are the 2.5th and 97.5th percentiles, whereas solid mid lines are the 50th percentile of the MCMC samples, respectively. Vertical gray line is the landmarking time. Predictions on the left-hand side of it are for serum creatinine, whereas on the right-hand side are for forecast probabilities. For the top-left panel, the lines on the left-hand side are replaced by dots; only the medians are displayed. See text for the patient characteristics.

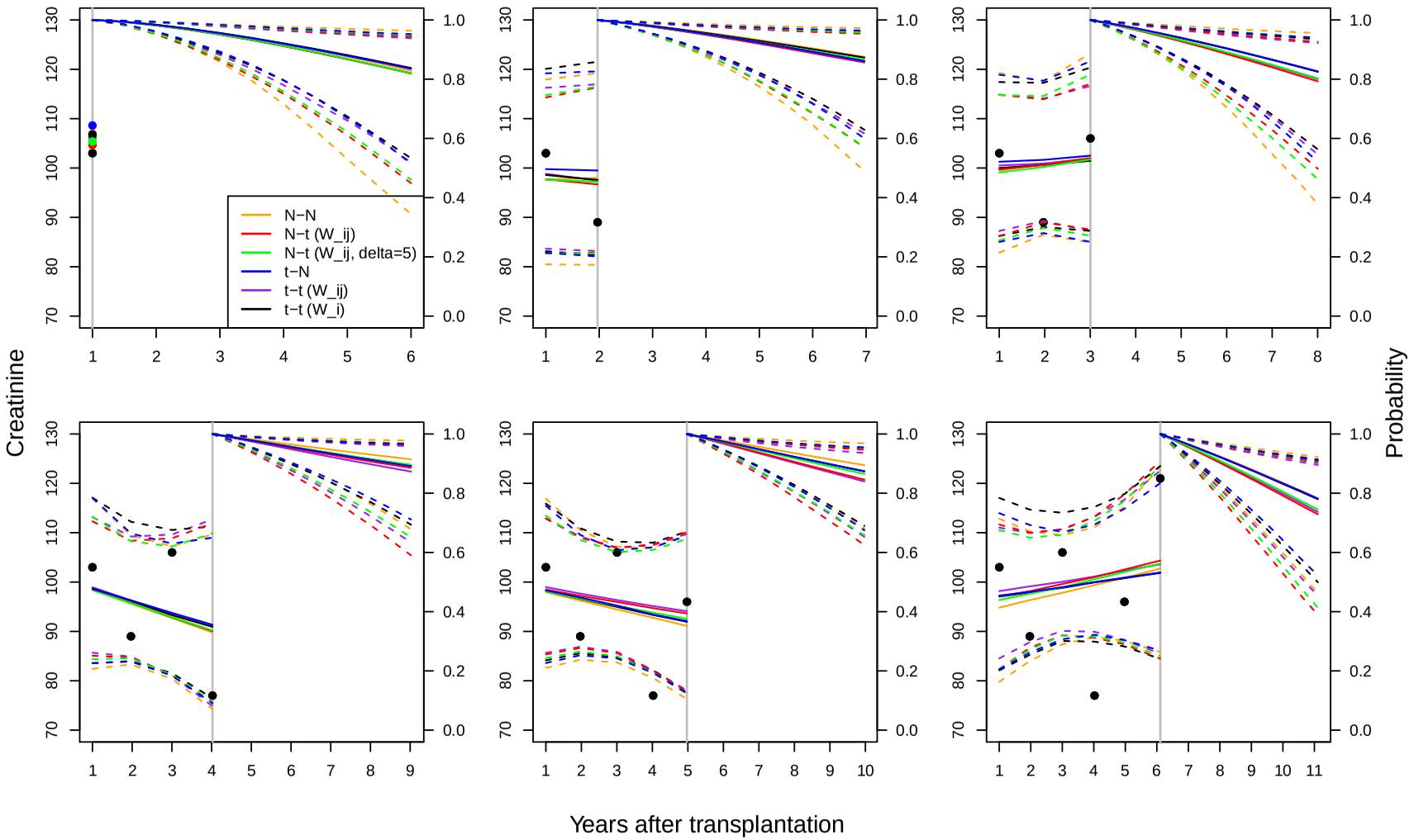


Figure 38: Dynamic predictions for the second person from the validation sample. Dots are observed data. Colours indicate different models; see the legend box in the upper-left panel. Dashed lower and upper lines are the 2.5th and 97.5th percentiles, whereas solid mid lines are the 50th percentile of the MCMC samples, respectively. Vertical gray line is the landmarking time. Predictions on the left-hand side of it are for serum creatinine, whereas on the right-hand side are for forecast probabilities. For the top-left panel, the lines on the left-hand side are replaced by dots; only the medians are displayed. See text for the patient characteristics.

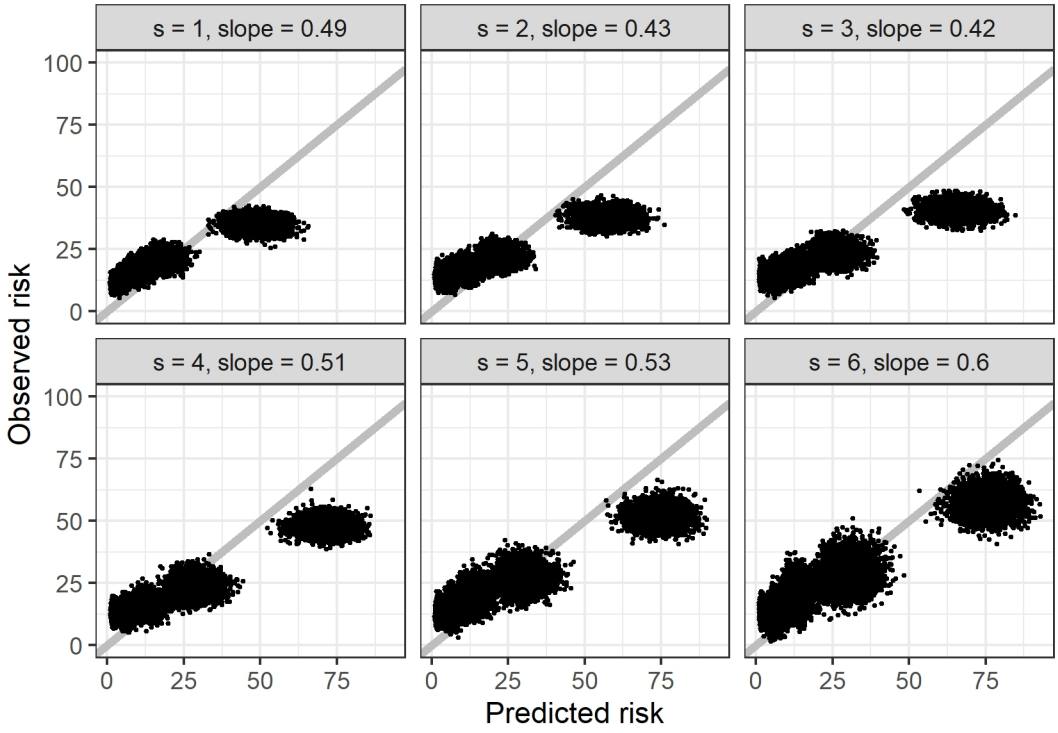


Figure 39: MCMC samples of the calibration plots based on the $N - N$ model across the landmark time-points for the external validation. Mean predicted risks and observed risks (Kaplan-Meier) are displayed for each subgroups defined by quintiles of prediction. Slope estimate is based on a simple linear regression fitted to the predicted and observed risk.

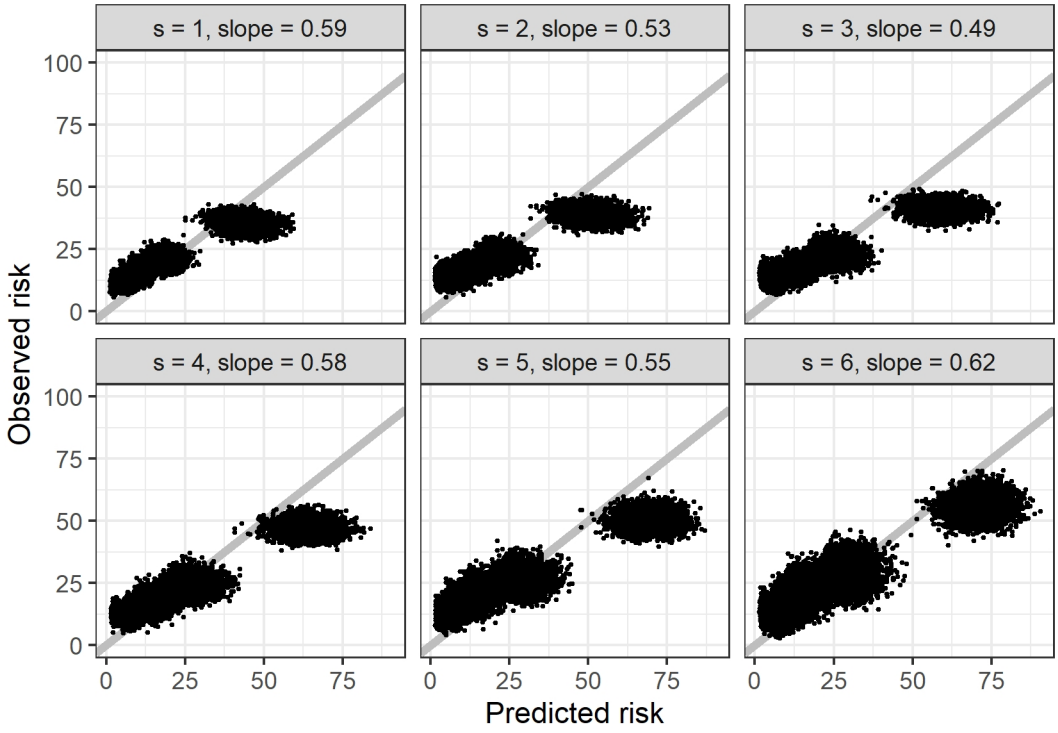


Figure 40: MCMC samples of the calibration plots based on the $N-t$ ($W_{ij}$) model across the landmark time-points for the external validation. Mean predicted risks and observed risks (Kaplan-Meier) are displayed for each subgroups defined by quintiles of prediction. Slope estimate is based on a simple linear regression fitted to the predicted and observed risk.

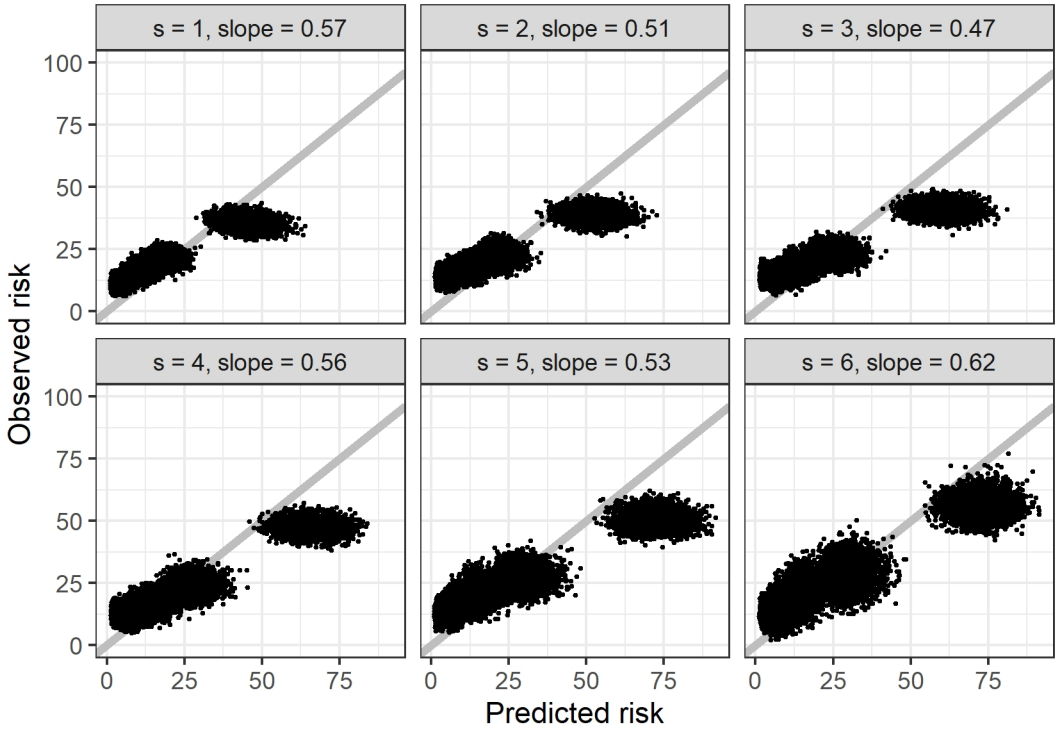


Figure 41: MCMC samples of the calibration plots based on the $N-t$ $(W_{ij}, \delta = 5)$ model across the landmark time-points for the external validation. Mean predicted risks and observed risks (Kaplan-Meier) are displayed for each subgroups defined by quintiles of prediction. Slope estimate is based on a simple linear regression fitted to the predicted and observed risk.

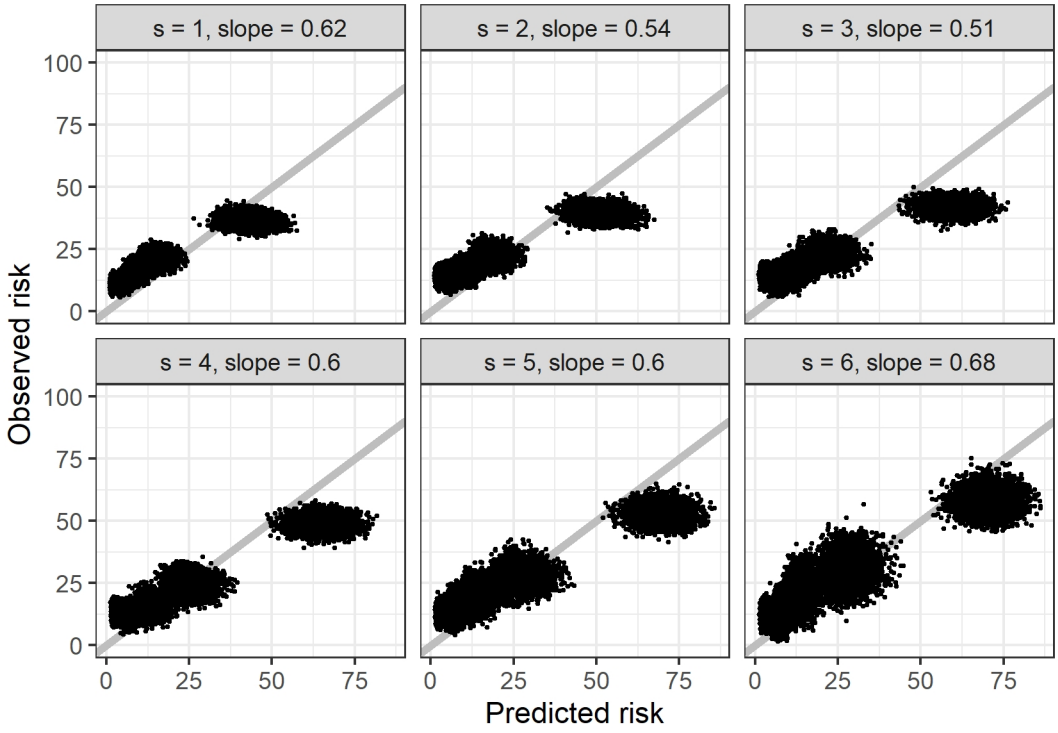


Figure 42: MCMC samples of the calibration plots based on the $t - N$ model across the landmark time-points for the external validation. Mean predicted risks and observed risks (Kaplan-Meier) are displayed for each subgroups defined by quintiles of prediction. Slope estimate is based on a simple linear regression fitted to the predicted and observed risk.

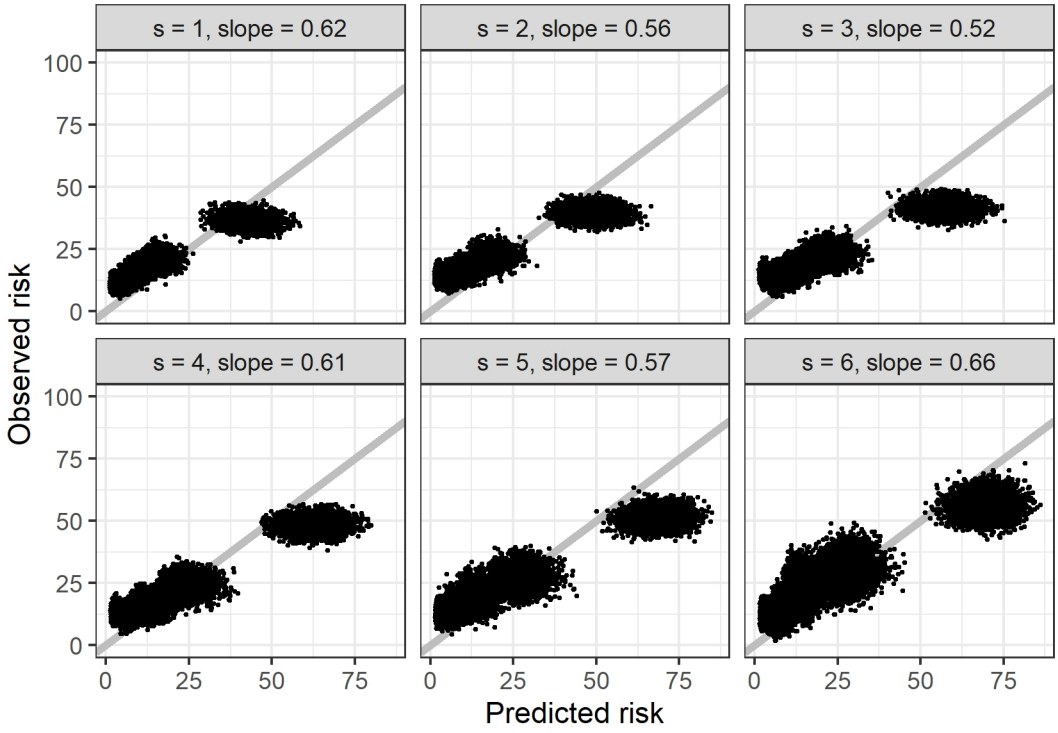


Figure 43: MCMC samples of the calibration plots based on the $t - t$ ($W_i$) model across the landmark time-points for the external validation. Mean predicted risks and observed risks (Kaplan-Meier) are displayed for each subgroups defined by quintiles of prediction. Slope estimate is based on a simple linear regression fitted to the predicted and observed risk.

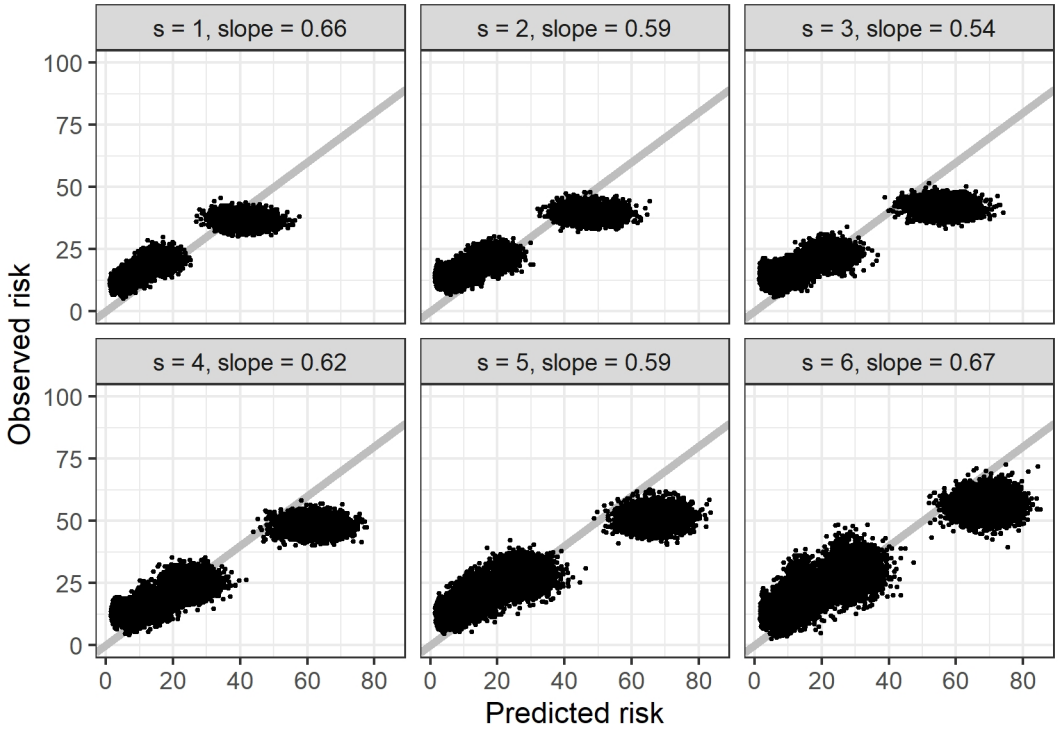


Figure 44: MCMC samples of the calibration plots based on the $t-t$ ($W_{ij}$) model across the landmark time-points for the external validation. Mean predicted risks and observed risks (Kaplan-Meier) are displayed for each subgroups defined by quintiles of prediction. Slope estimate is based on a simple linear regression fitted to the predicted and observed risk.

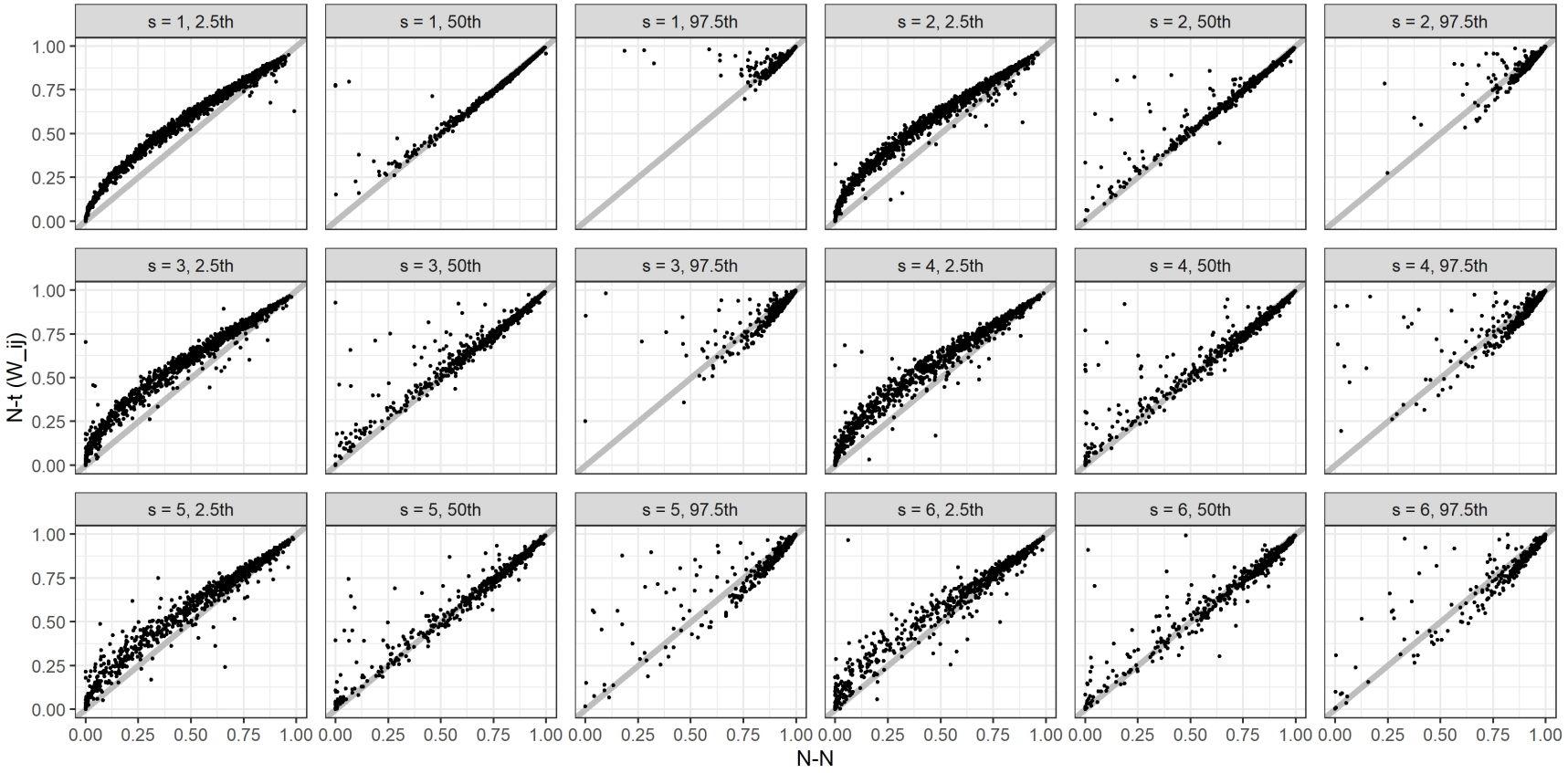


Figure 45: Scatter-plots of the 2.5th, 50th and 97.5th quantiles of the dynamic predictions across landmark time-points ($s = 1, 2, 3, 4, 5, 6$) for the external validation. x-axis is the $N - N$ model, y-axis the $N - t$ ($W_{ij}$). Gray lines are $x = y$ lines.

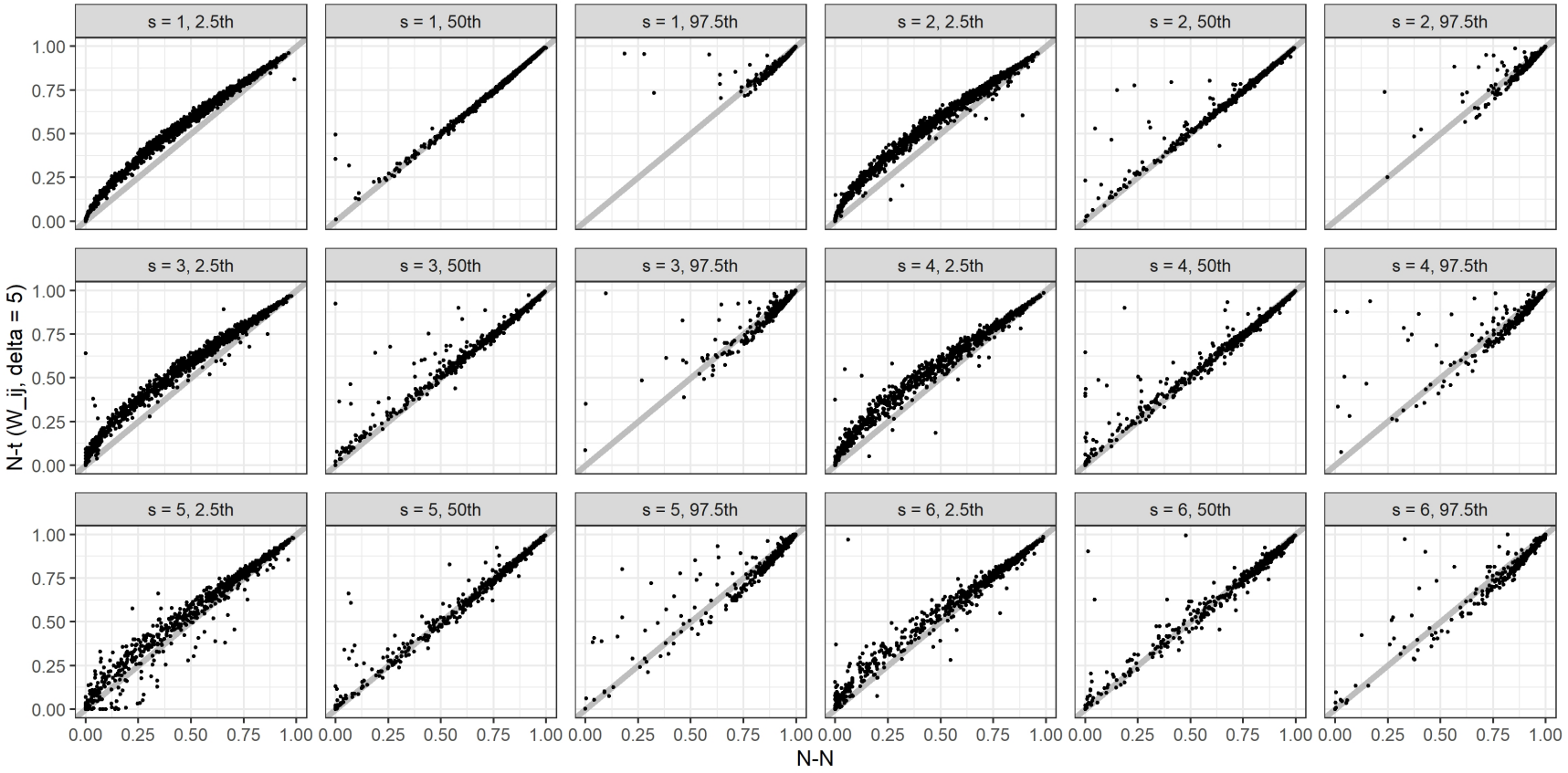


Figure 46: Scatter-plots of the 2.5th, 50th and 97.5th quantiles of the dynamic predictions across landmark time-points ($s = 1, 2, 3, 4, 5, 6$) for the external validation. x-axis is the $N - N$ model, y-axis the $N - t$ ($W_{ij}, \delta = 5$). Gray lines are $x = y$ lines.

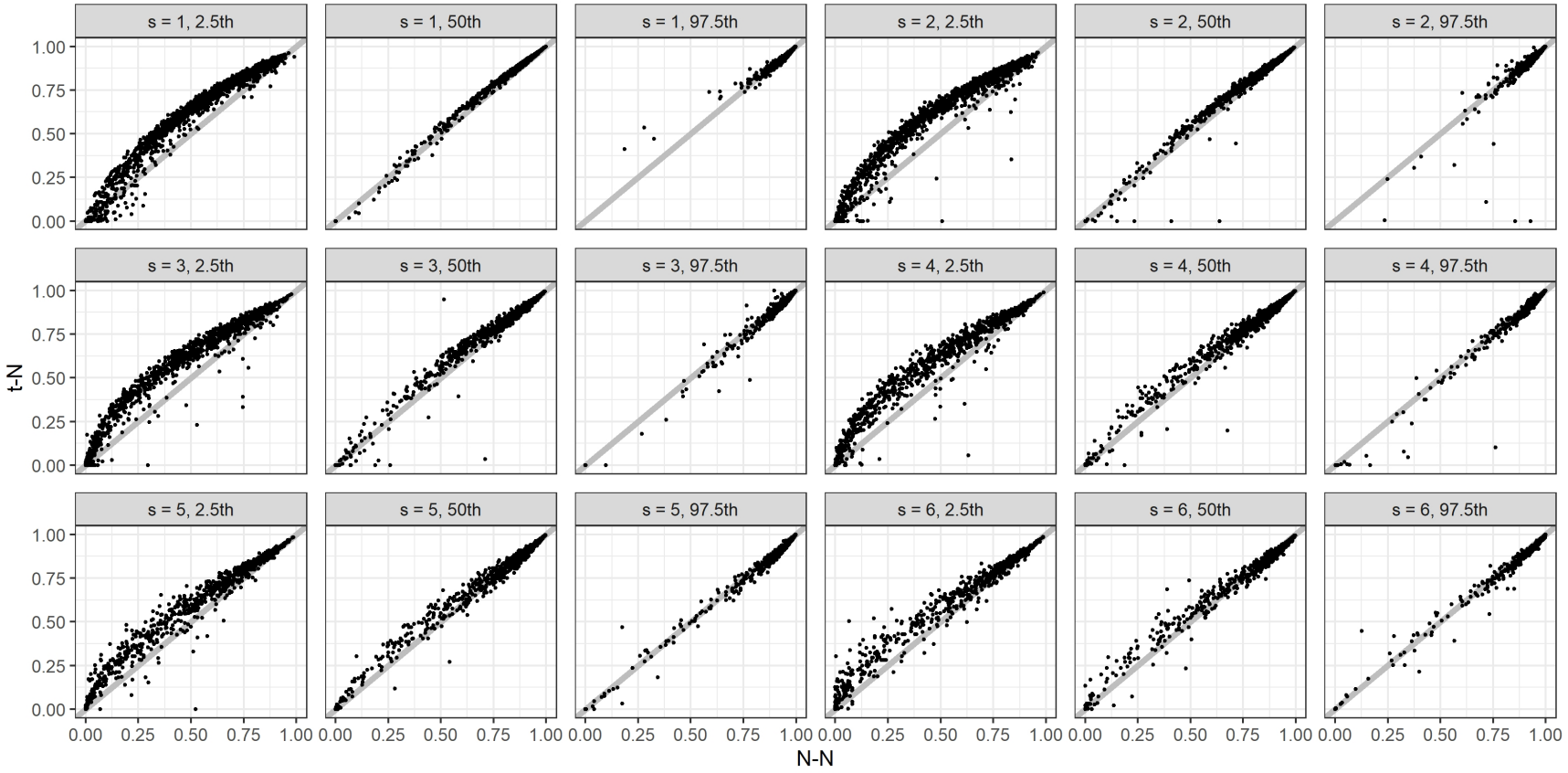


Figure 47: Scatter-plots of the 2.5th, 50th and 97.5th quantiles of the dynamic predictions across landmark time-points ($s = 1, 2, 3, 4, 5, 6$) for the external validation. x-axis is the $N - N$ model, y-axis the $N - t$. Gray lines are $x = y$ lines.

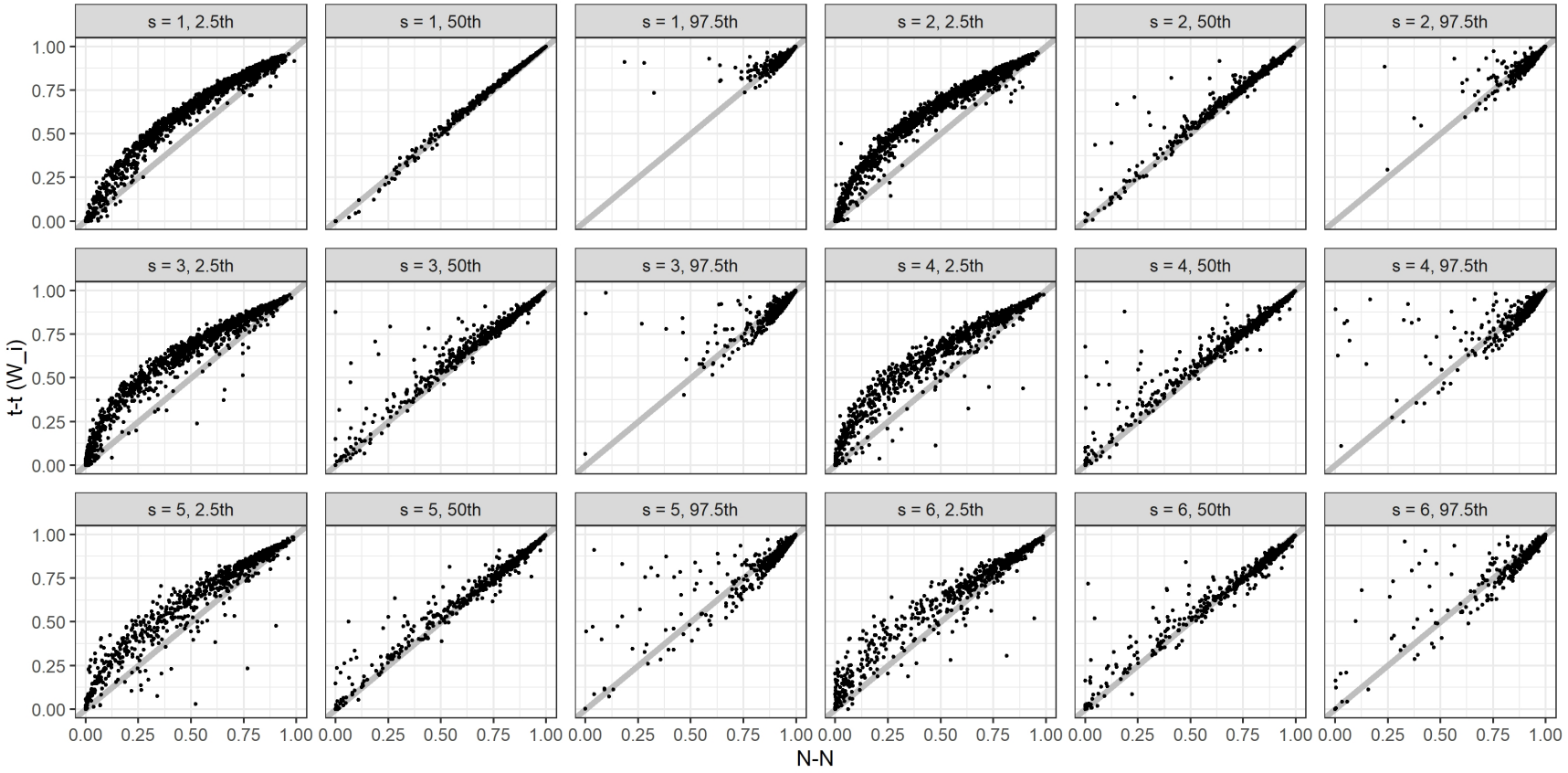


Figure 48: Scatter-plots of the 2.5th, 50th and 97.5th quantiles of the dynamic predictions across landmark time-points ($s = 1, 2, 3, 4, 5, 6$) for the external validation. x-axis is the $N - N$ model, y-axis the $t - t$ ($W_i$). Gray lines are $x = y$ lines.

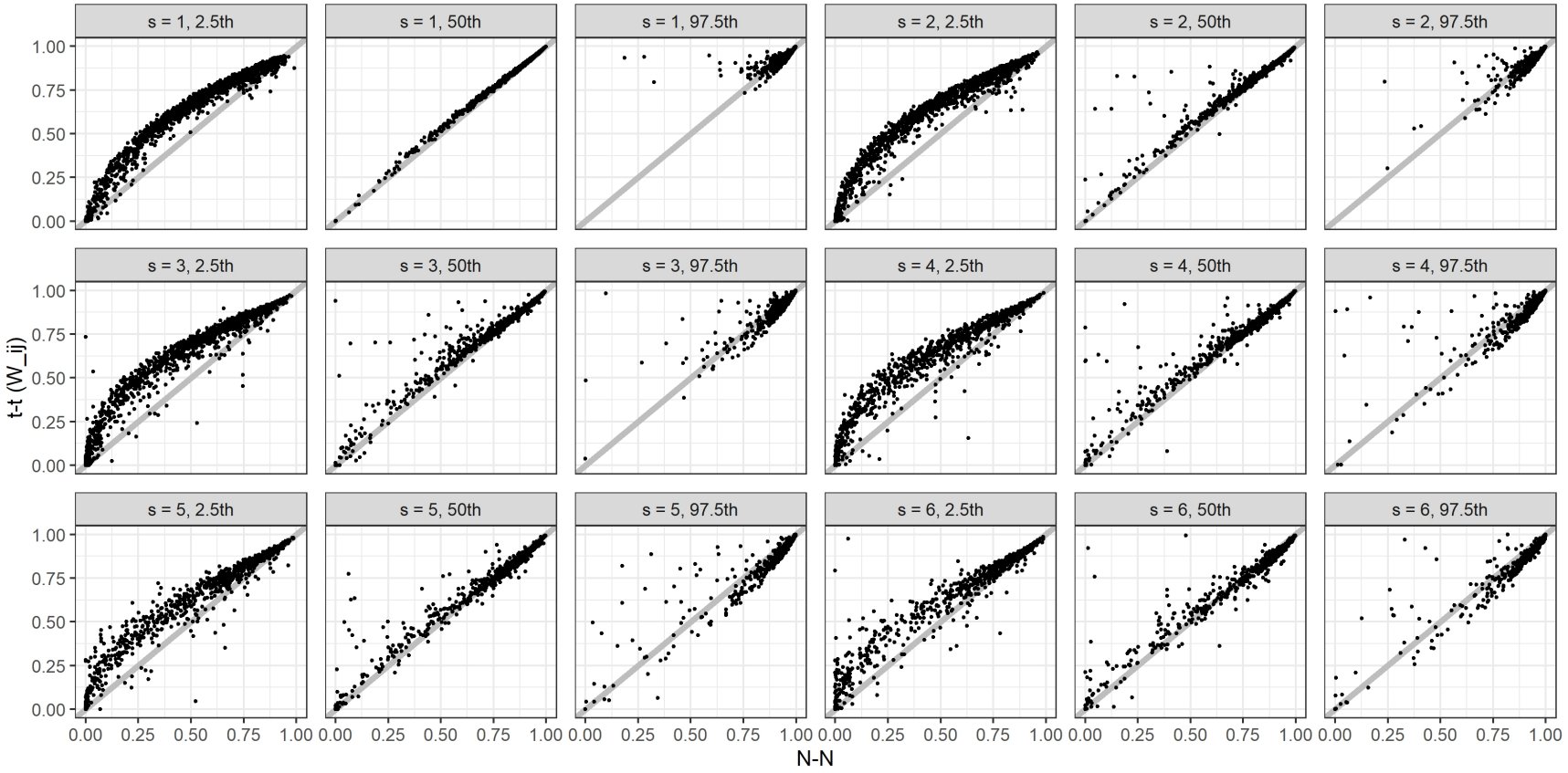


Figure 49: Scatter-plots of the 2.5th, 50th and 97.5th quantiles of the dynamic predictions across landmark time-points ($s = 1, 2, 3, 4, 5, 6$) for the external validation. x-axis is the $N - N$ model, y-axis the $t - t$ ($W_{ij}$). Gray lines are $x = y$ lines.

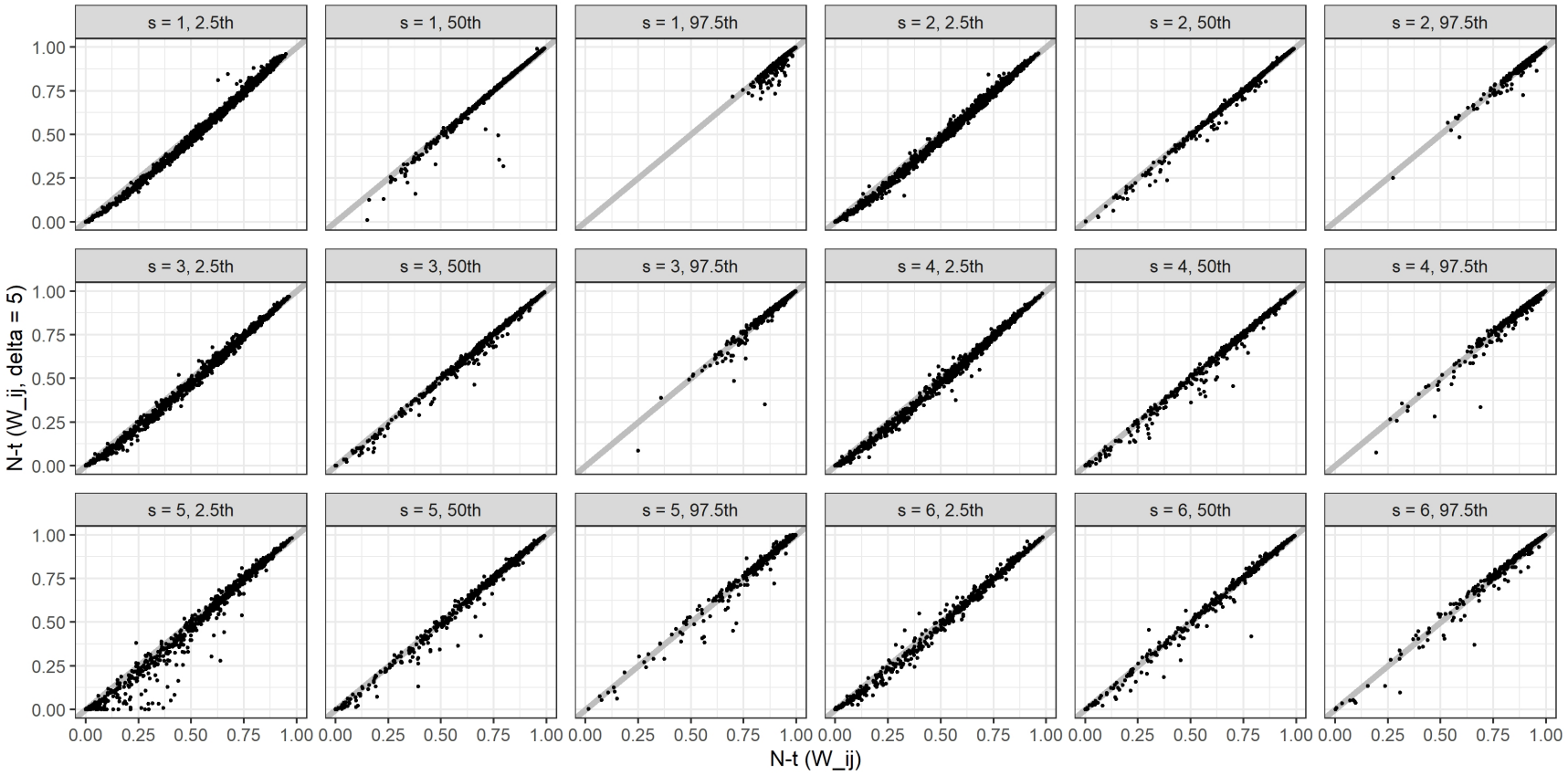


Figure 50: Scatter-plots of the 2.5th, 50th and 97.5th quantiles of the dynamic predictions across landmark time-points ($s = 1, 2, 3, 4, 5, 6$) for the external validation. x-axis is the $N - t$ $(W_{ij})$ model, y-axis the $N - t$ $(W_{ij}, \delta = 5)$. Gray lines are $x = y$ lines.

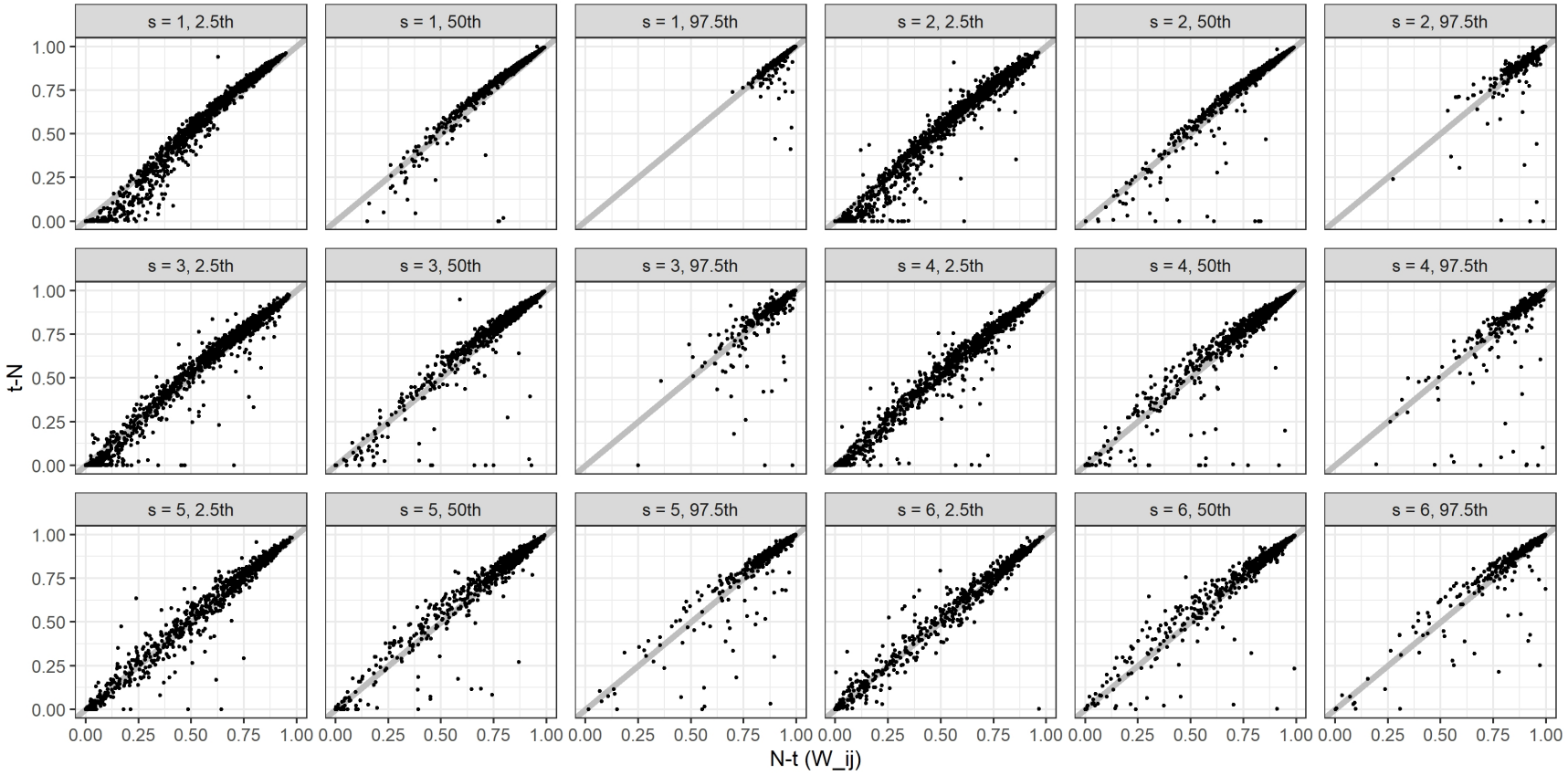


Figure 51: Scatter-plots of the 2.5th, 50th and 97.5th quantiles of the dynamic predictions across landmark time-points ($s = 1, 2, 3, 4, 5, 6$) for the external validation. x-axis is the $N - t$ ($W_{ij}$) model, y-axis the $t - N$. Gray lines are $x = y$ lines.

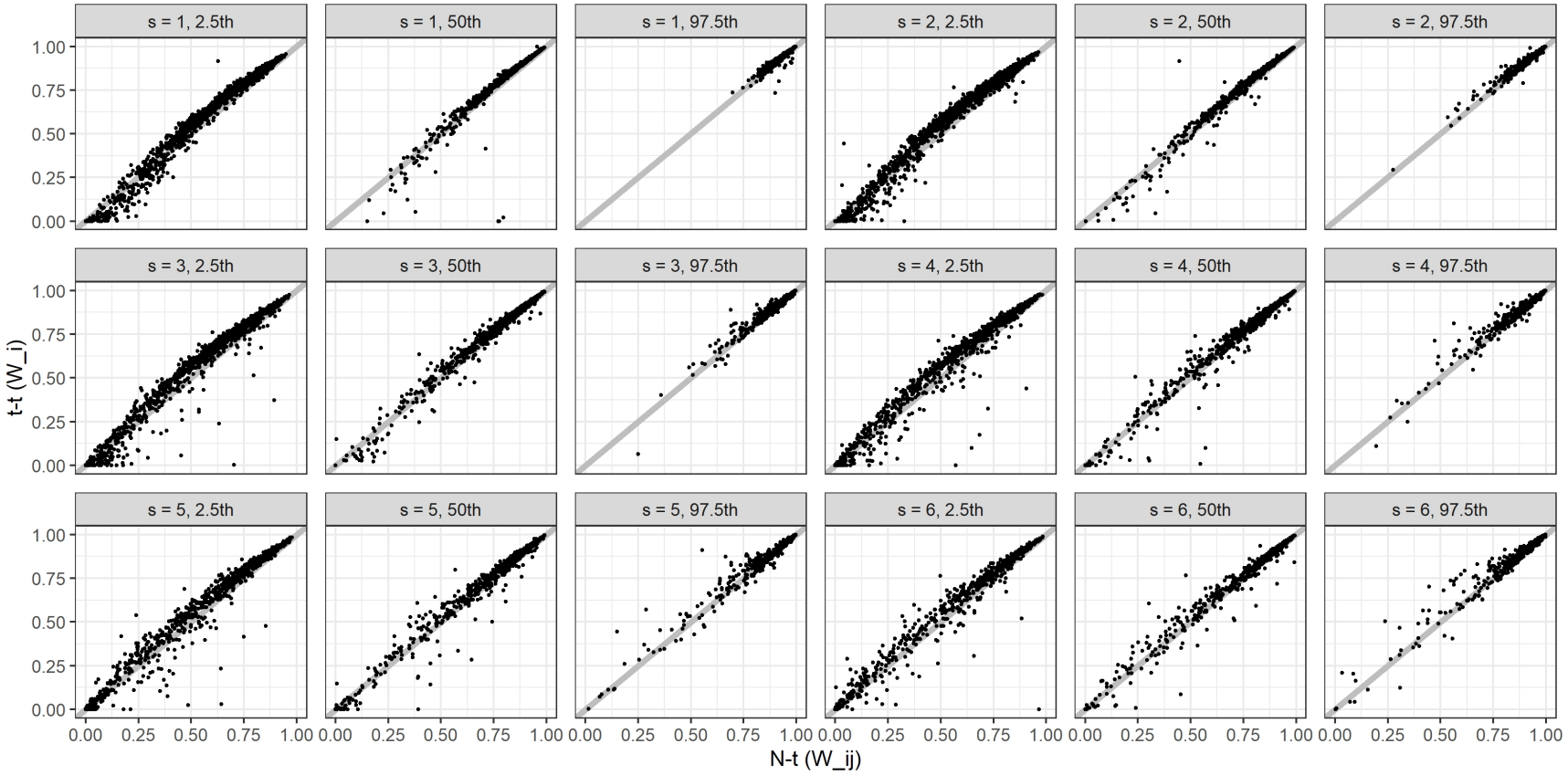


Figure 52: Scatter-plots of the 2.5th, 50th and 97.5th quantiles of the dynamic predictions across landmark time-points ($s = 1, 2, 3, 4, 5, 6$) for the external validation. x-axis is the $N - t$ ($W_{ij}$) model, y-axis the $t - t$ ($W_i$). Gray lines are $x = y$ lines.

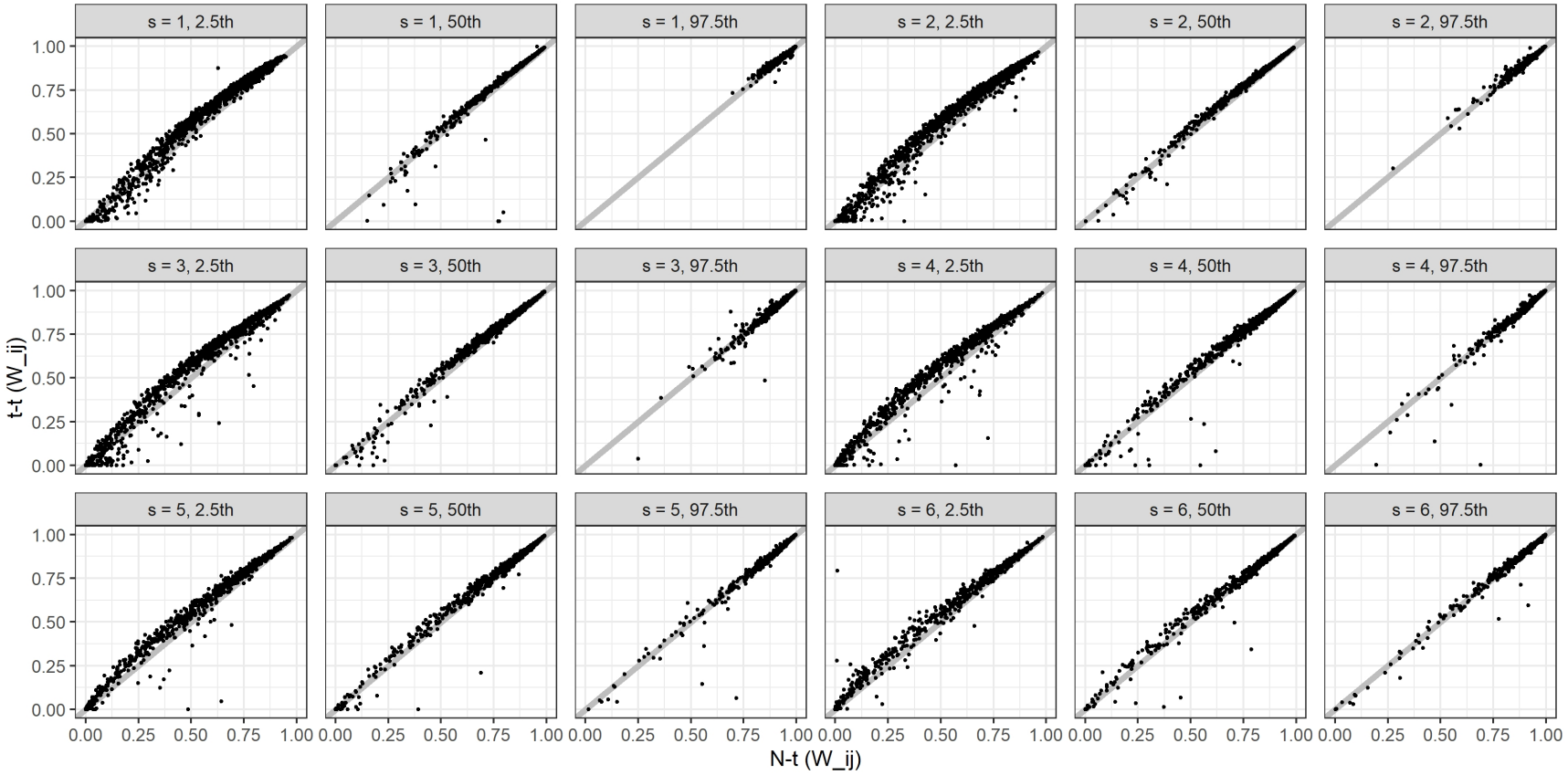


Figure 53: Scatter-plots of the 2.5th, 50th and 97.5th quantiles of the dynamic predictions across landmark time-points ($s = 1, 2, 3, 4, 5, 6$) for the external validation. x-axis is the $N - t$ ($W_{ij}$) model, y-axis the $t - t$ ($W_{ij}$). Gray lines are $x = y$ lines.

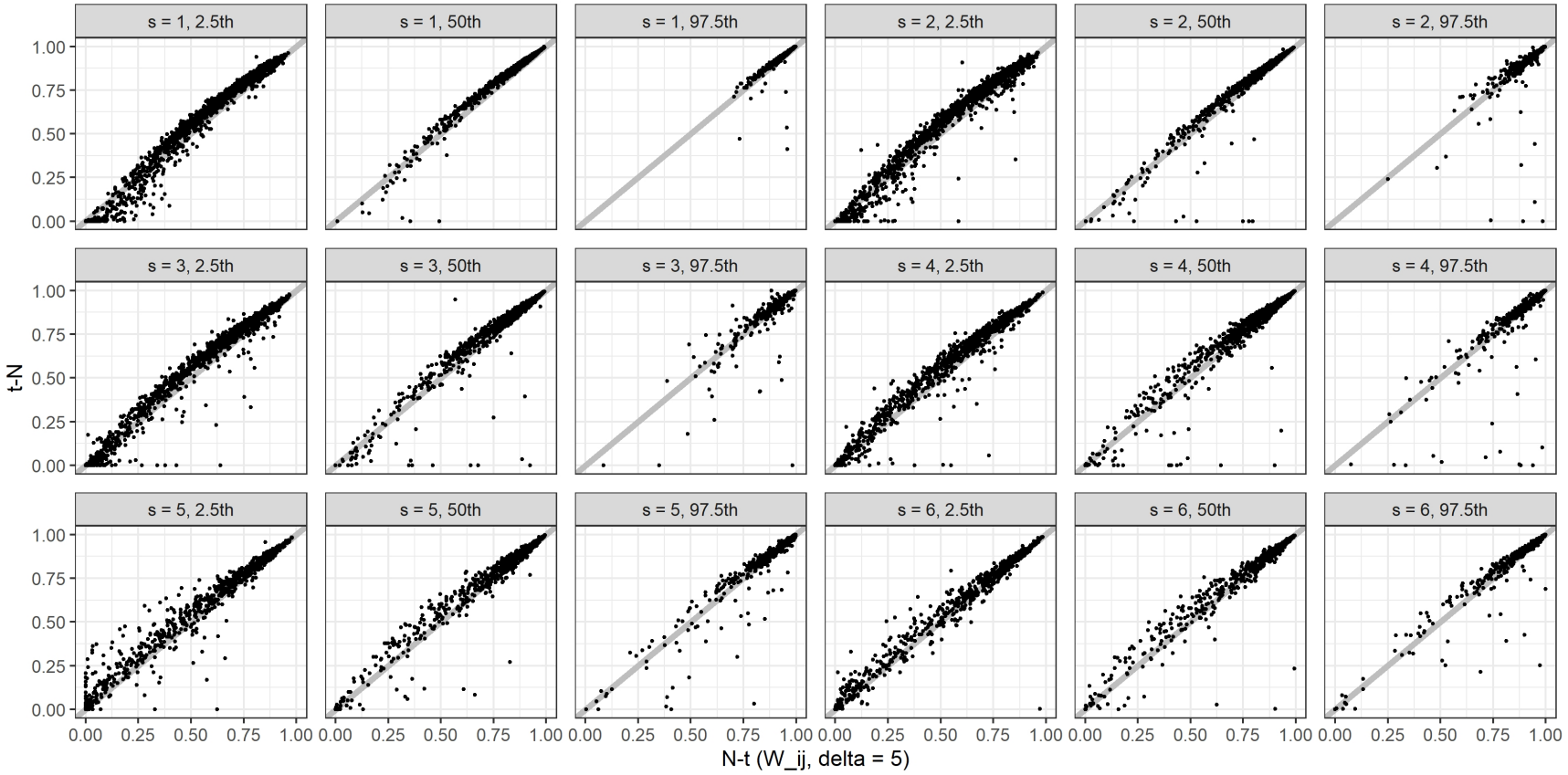


Figure 54: Scatter-plots of the 2.5th, 50th and 97.5th quantiles of the dynamic predictions across landmark time-points ($s = 1, 2, 3, 4, 5, 6$) for the external validation. x-axis is the $N - t$ $(W_{ij}, \delta = 5)$ model, y-axis the $t - N$. Gray lines are $x = y$ lines.

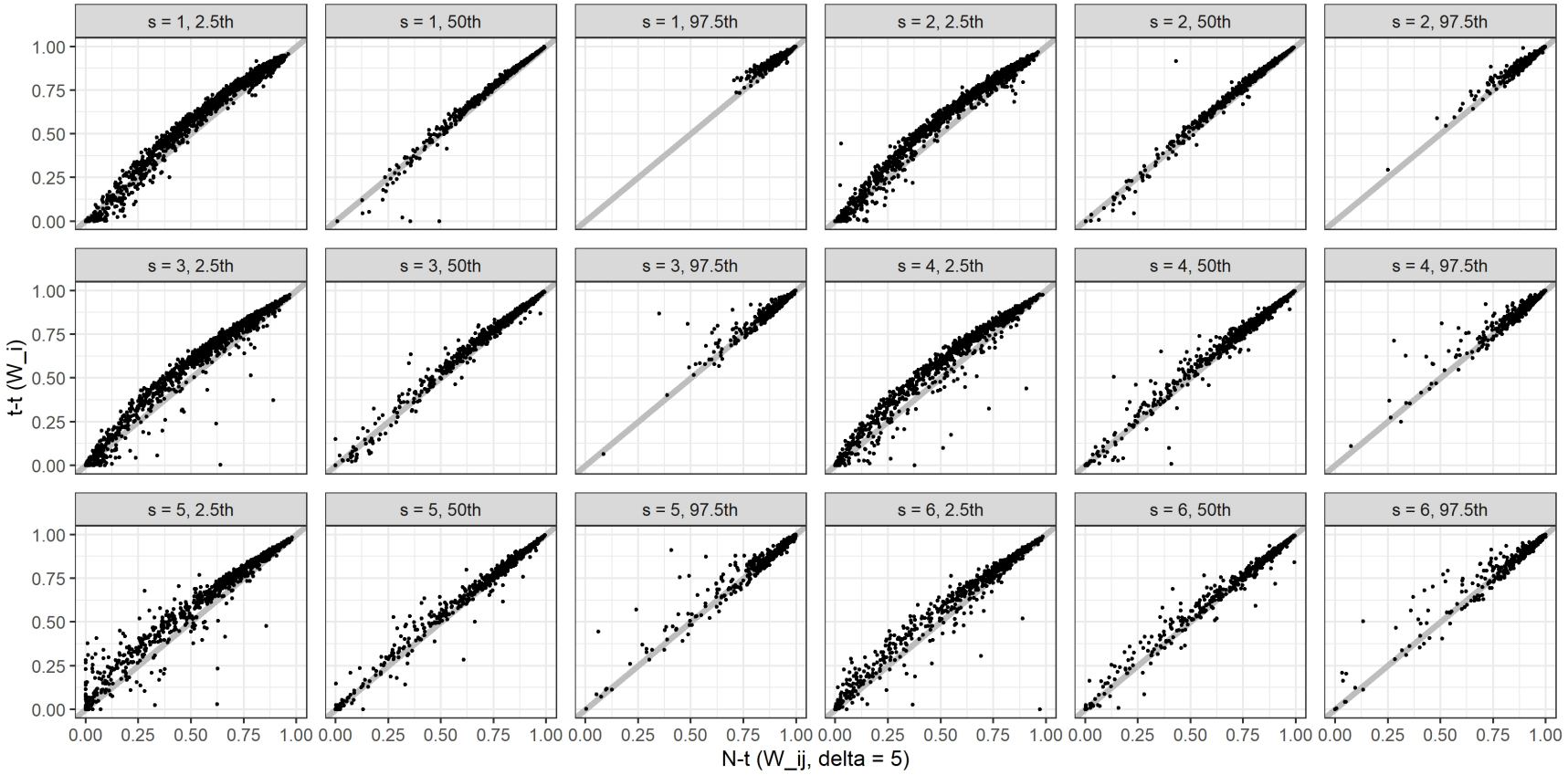


Figure 55: Scatter-plots of the 2.5th, 50th and 97.5th quantiles of the dynamic predictions across landmark time-points ($s = 1, 2, 3, 4, 5, 6$) for the external validation. x-axis is the $N - t$ $(W_{ij}, \delta = 5)$ model, y-axis the $t - t$ $(W_i)$. Gray lines are $x = y$ lines.

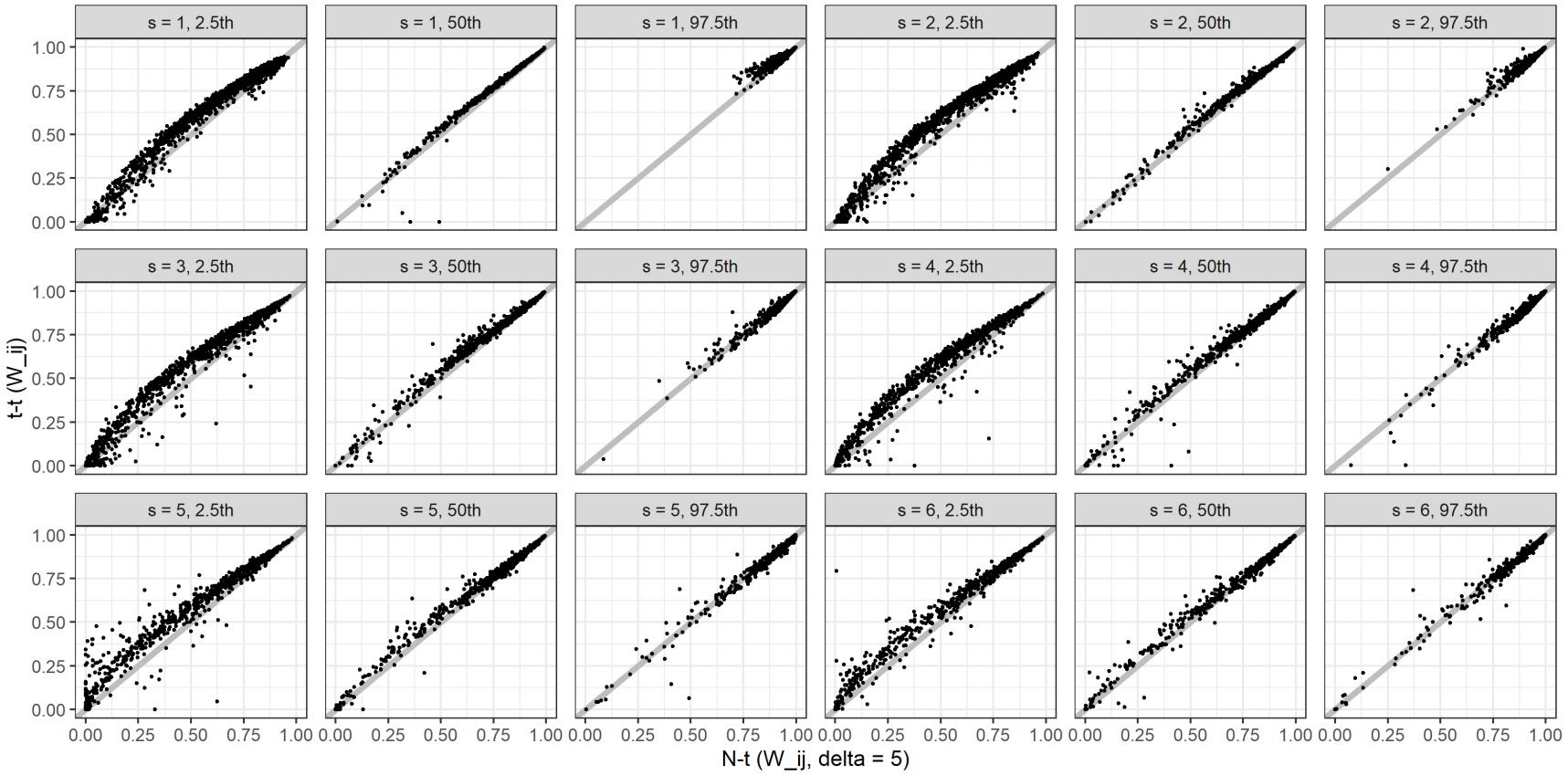


Figure 56: Scatter-plots of the 2.5th, 50th and 97.5th quantiles of the dynamic predictions across landmark time-points ($s = 1, 2, 3, 4, 5, 6$) for the external validation. x-axis is the $N - t$ $(W_{ij}, \delta = 5)$ model, y-axis the $t - t$ $(W_{ij})$. Gray lines are $x = y$ lines.

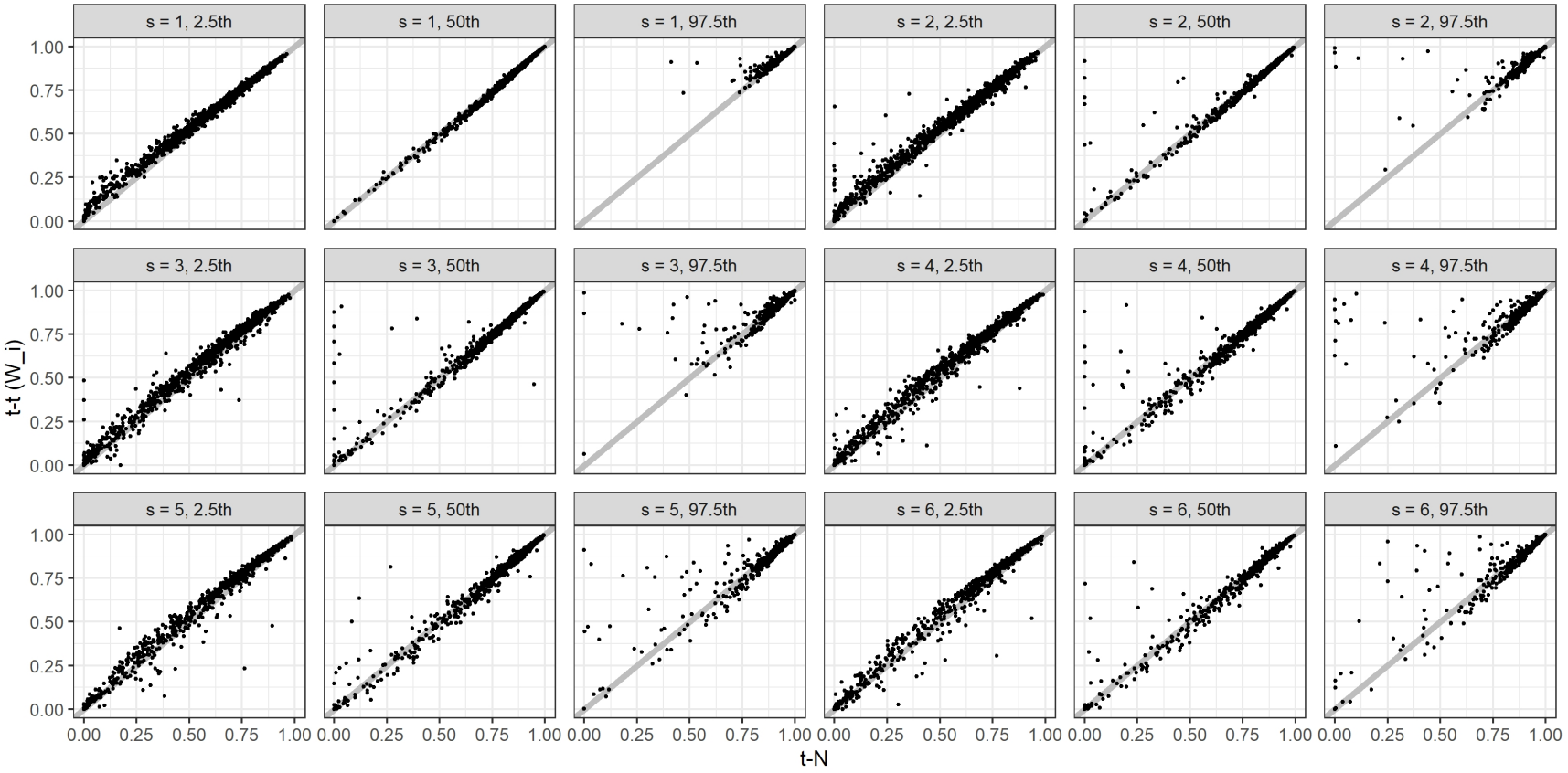


Figure 57: Scatter-plots of the 2.5th, 50th and 97.5th quantiles of the dynamic predictions across landmark time-points ($s = 1, 2, 3, 4, 5, 6$) for the external validation. x-axis is the $t - N$ model, y-axis the $t - t$ ($W_i$). Gray lines are $x = y$ lines.

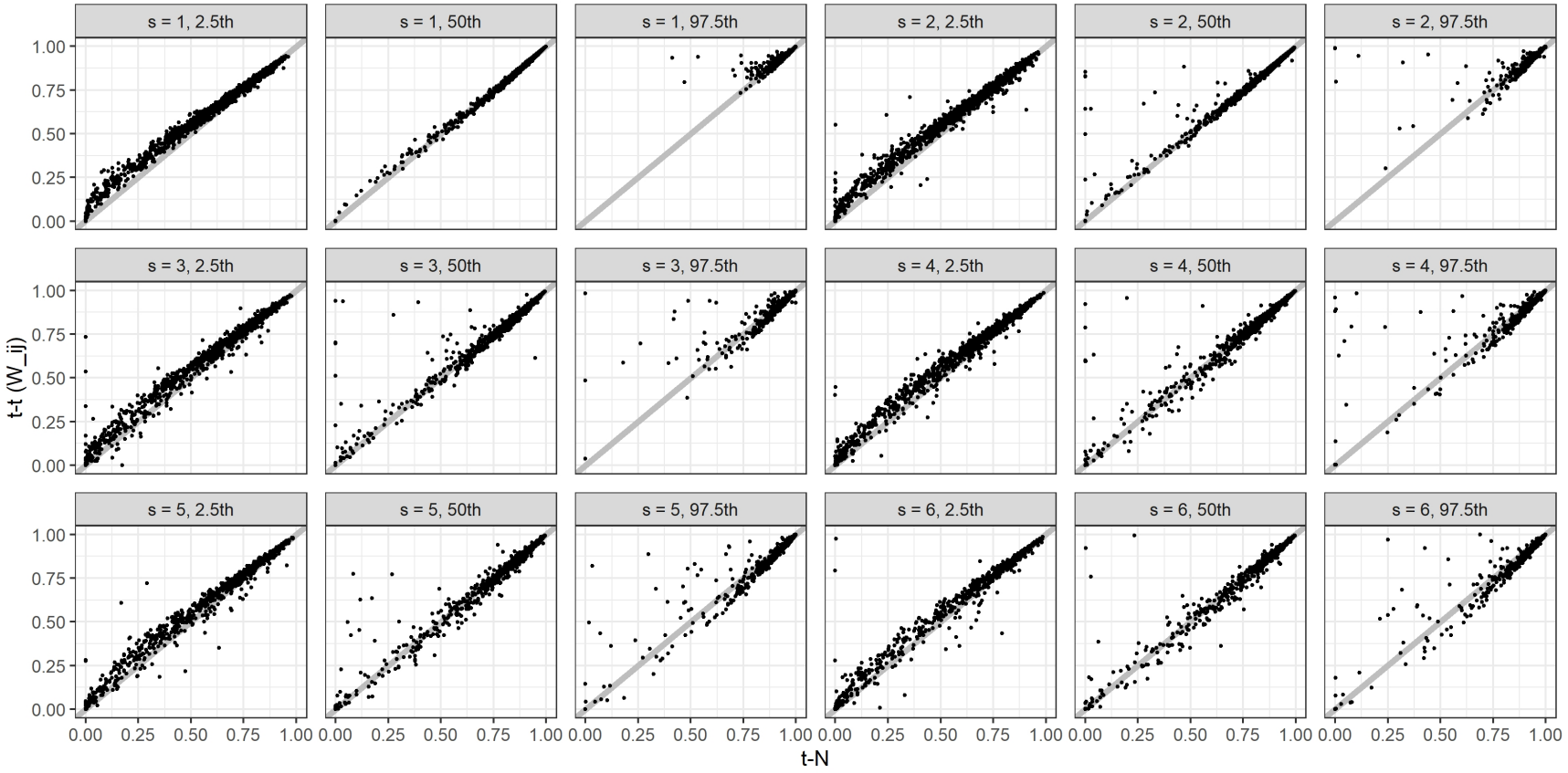


Figure 58: Scatter-plots of the 2.5th, 50th and 97.5th quantiles of the dynamic predictions across landmark time-points ($s = 1, 2, 3, 4, 5, 6$) for the external validation. x-axis is the $t - N$ model, y-axis the $t - t$ ($W_{ij}$). Gray lines are $x = y$ lines.

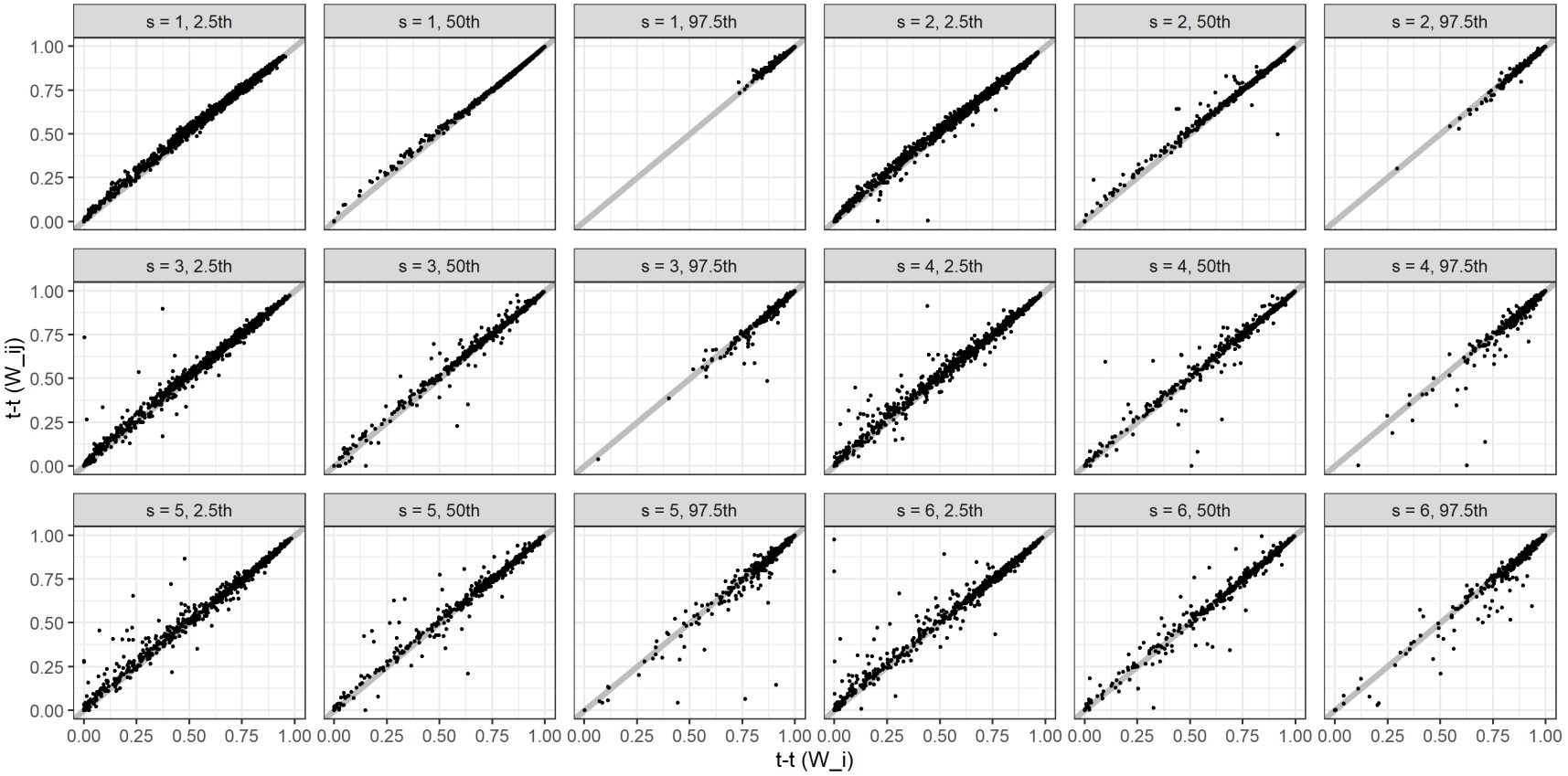


Figure 59: Scatter-plots of the 2.5th, 50th and 97.5th quantiles of the dynamic predictions across landmark time-points ($s = 1, 2, 3, 4, 5, 6$) for the external validation. x-axis is the $t - t$ ($W_i$) model, y-axis the $t - t$ ($W_{ij}$). Gray lines are $x = y$ lines.

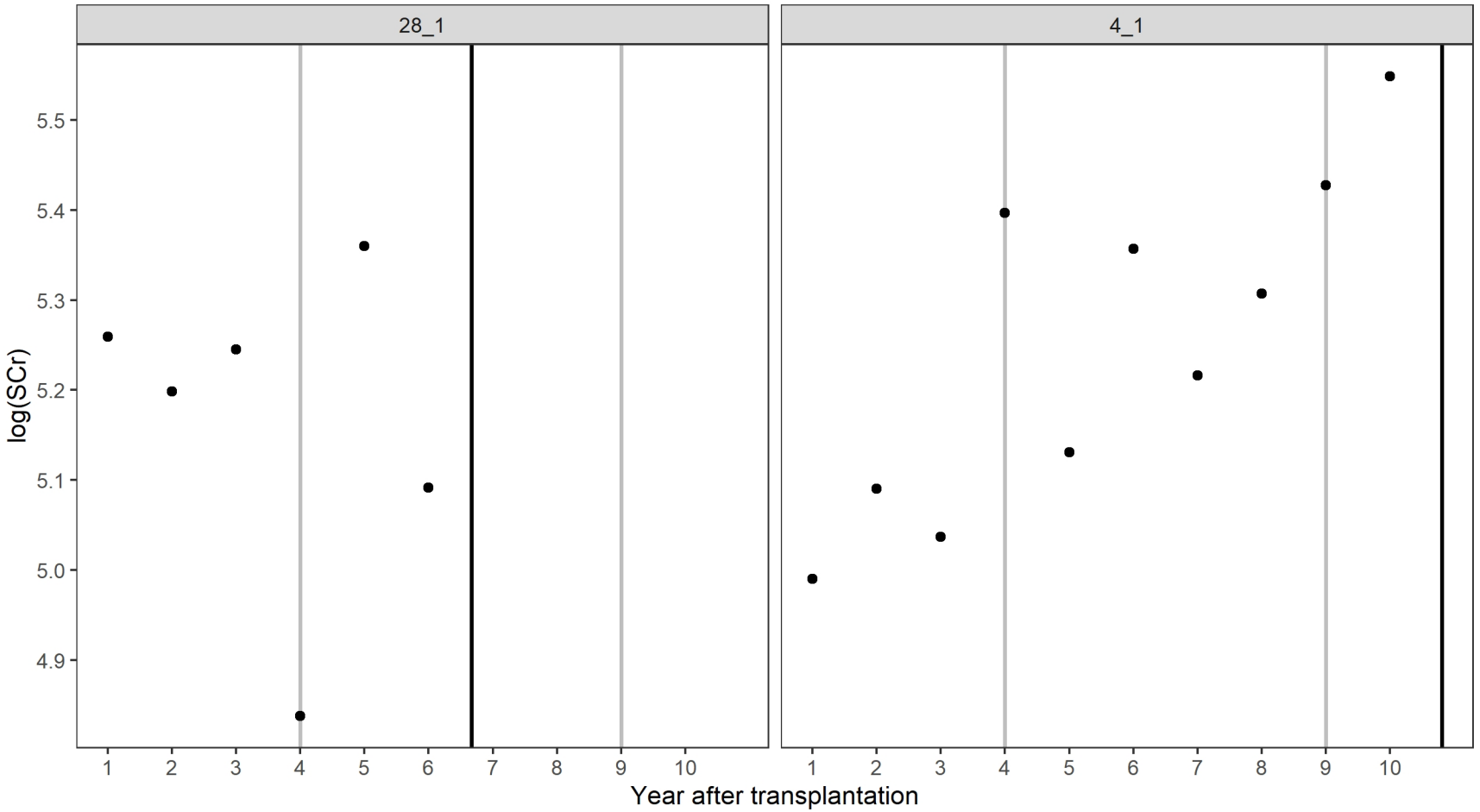


Figure 60: Two subjects from the simulation study; $N - N$ is the simulation model. Dots are observed log-transformed serum creatinine (SCr) measurements. Two vertical gray lines indicate landmark time point, $s = 4$, and landmark time point plus the forecast horizon, $s + u = 9$. Solid black line indicate the true survival times, $T^*$. Note that SCr measurements that occur after $s = 4$ are discarded. 4th repeats of both of the subjects act as outlying observations. The median (2.5% and 97.50% percentiles of the) conditional survival probability forecasts of $T^* > 9$ under the $N - N$ and $t - t$ ($W_{ij}$) models are 0.61 (0.14, 0.88) and 0.38 (0.03, 0.82), respectively, for the subject with ID = 28_1 (left panel), and 0.06 (0.000001, 0.52) and 0.17 (0.0002, 0.57), respectively, for the one with ID = 4_1 (right panel). Note that lower survival probability for for the subject with ID = 28_1 is better, whereas higher is better for the other subject.